AGU ADVANCING EARTH AND SPACE SCIENCES

Water Resources Research

RESEARCH ARTICLE
10.1029/2023WR036996

Identifying Canopy Snow in Subalpine Forests: A Comparative Study of Methods

Natasha Harvey[1,2], Sean P. Burns[1,3], Keith N. Musselman[1,4], Holly Barnard[1,4], and Peter D. Blanken[1]

[1]Department of Geography, University of Colorado, Boulder, CO, USA, [2]Fenner School of Environment and Society, Australian National University, Canberra, ACT, Australia, [3]NSF National Center for Atmospheric Research, Boulder, CO, USA, [4]Institute of Arctic and Alpine Research, University of Colorado, Boulder, CO, USA

Key Points:

- Snow interception in subalpine forests, identified via flux measurements, imagery and models, indicates its significance
- Convolutional Neural Network models trained with Phenocam imagery offer insights into snow interception beyond model development period
- Consider data availability and research goals when choosing a method to estimate the presence of snow interception

Supporting Information:

Supporting Information may be found in the online version of this article.

Correspondence to:

N. Harvey,
natasha.harvey@colorado.edu

Citation:

Harvey, N., Burns, S. P., Musselman, K. N., Barnard, H., & Blanken, P. D. (2025). Identifying canopy snow in subalpine forests: A comparative study of methods. *Water Resources Research*, *61*, e2023WR036996. https://doi.org/10.1029/2023WR036996

Received 22 DEC 2023
Accepted 21 DEC 2024

Author Contributions:

Conceptualization: Natasha Harvey, Keith N. Musselman, Holly Barnard, Peter D. Blanken
Formal analysis: Natasha Harvey
Funding acquisition: Peter D. Blanken
Methodology: Natasha Harvey, Sean P. Burns
Software: Natasha Harvey
Supervision: Sean P. Burns, Keith N. Musselman, Holly Barnard, Peter D. Blanken
Visualization: Natasha Harvey
Writing – original draft: Natasha Harvey
Writing – review & editing: Natasha Harvey, Sean P. Burns, Keith N. Musselman, Holly Barnard, Peter D. Blanken

Abstract The interception of snow by the canopy is an important process in the water and energy balance in cold-region coniferous forests. Direct measurements of canopy snow interception are difficult at scales larger than individual trees, requiring indirect methods such as eddy covariance, time-lapse photography, or modeling. At the Niwot Ridge Subalpine Forest AmeriFlux site in the Colorado Front Range, USA, we compared methods that estimate or simulate the presence of snow interception. Timelapse photography images were analyzed using thresholding analysis and used to train a Convolutional Neural Network (CNN) model to estimate canopy snow presence. Interception was also estimated from eddy covariance measurements above and below the canopy, as well as from model simulations. These methods were applied over January 2019, with binarized results compared to a "ground truth" of human labeled images to calculate the Balanced Accuracy Score. The highest accuracy was achieved by the CNN predictions. Based on the Balanced Accuracy Scores, select methods were extended to estimate the presence of canopy snow for the 2018/2019 winter. All methods provided insight into the process of interception in a subalpine forest but presented challenges, including differing flux footprints of the above- and below-canopy eddy covariance measurements and the inability of red-green-blue imagery to monitor snow interception at night, during sunrise, and during sunset.

1. Introduction

The interception and presence of snow in a forest canopy is an important process in cold-region coniferous forests, creating conditions for sublimation from the canopy, influencing albedo, and altering the water and energy balances (Bartlett & Verseghy, 2015; Gutmann, 2020; Lundquist et al., 2024; Pomeroy & Schmidt, 1993; Stähli et al., 2009; Strasser et al., 2008; Suzuki & Nakai, 2008). In forested environments, up to 60% of winter snowfall can be intercepted (Pomeroy & Schmidt, 1993), with sublimation from intercepted snow dominating over other alternate sublimation pathways such as from the snowpack or blowing snow (Frank et al., 2019; Molotch et al., 2007; Strasser et al., 2008). However, snow interception is difficult to measure in-situ beyond the point scale (i.e., a single tree) (Lundberg & Halldin, 1994; Montesi et al., 2004; Nakai et al., 1994; Raleigh et al., 2022), necessitating the development of models to simulate interception (Hedstrom & Pomeroy, 1998; Lv & Pomeroy, 2019; Niu et al., 2011; Roesch et al., 2001; Strasser et al., 2008). Models can also be used to understand which processes influence snow interception and subsequent unloading via wind, melting, or sublimation (Hedstrom & Pomeroy, 1998; Lumbrazo et al., 2022; Roesch et al., 2001). It is common to validate or evaluate a model against observations (Beven, 2005), however, the lack of interception measurements hinders efforts to validate interception algorithms used in land surface models (Lundquist et al., 2021).

One approach to identify the presence of snow interception is by measuring sublimation losses from intercepted snow. This can be done by comparing water vapor flux measurements using the eddy covariance method at two heights: one below the canopy to measure sublimation losses from the ground snowpack and one above the canopy to measure sublimation losses from both the snowpack surface and canopy-intercepted snow (Mahat et al., 2013; Molotch et al., 2007). By subtracting these two measurements, sublimation of intercepted snow is estimated (Mahat et al., 2013; Molotch et al., 2007), which can serve as a proxy for snow interception (i.e., the difference should only be greater than zero when there is intercepted snow available to sublimate and there is no transpiration). This method does not determine how much snow is intercepted, as not all intercepted snow is destined to sublimate (some intercepted snow will unload), but serves as a useful indicator of when snow is present on the canopy.

Alternatively, time-lapse photography has the potential to be a useful, low-cost method to continuously monitor complex snow processes such as canopy interception in forested environments, particularly at spatial scales larger than individual trees (Dong & Menzel, 2017; Floyd & Weiler, 2008; Garvelmann et al., 2013; Parajka et al., 2012). The images produced by Parajka et al. (2012) proved useful as a simple validation of an interception model but could not be used to estimate the mass of intercepted snow. Dong and Menzel (2017) calculated the canopy intercepted snow in forested sites on the French-German border by testing different classification techniques and employing a snow interception index based on the number of pixels identified as snow versus the total number of pixels in the image. Lumbrazo et al. (2022) compared snow interception observations from photographs classified by citizen scientists to model estimates (Andreadis et al., 2009; Hedstrom & Pomeroy, 1998; Roesch et al., 2001) at three sites in the Western US. The study found that models underestimated snow interception in warm environments, where winter air temperatures frequently exceed 0°C, but overestimated interception duration and simulated interception when none was observed in cold environments (Lumbrazo et al., 2022). More recently, low-cost accelerometers attached to trees have been used to quantify snow interception based on tree sway frequency (Raleigh et al., 2022).

Motivated by these past studies that demonstrate the importance of canopy intercepted snow in cold region coniferous forest environments, coupled with the need to extrapolate these measurements spatially and temporally while also evaluating models, we present a study of snow interception in a coniferous subalpine forest. Our research objectives are: (a) to compare different methods - time-lapse photography, eddy covariance and models - that assess the presence and timing of interception throughout January 2019; (b) compare the methods to a "ground truth" of human labeled images and calculate a common statistic; and (c) extend the best-performing methods for snow interception detection to the 2018/2019 winter.

2. Study Site

The Niwot Ridge Forest AmeriFlux site (US-NR1; 40.0329, −105.5464; elevation: 3,050 m.a.s.l.; Figure 1) in the Como Creek catchment in the Rocky Mountains roughly 8 km east of the Continental Divide. This site was selected because snowmelt is a crucial water resource in this region (Adam et al., 2009) and it offers an array of measurements and long-term observations related to canopy and snow processes (Burns et al., 2015; Monson et al., 2002). There are also many other research sites in the general area providing ancillary data (Figure 1).

On average, snow is present at US-NR1 between October/November and May/June (Burns et al., 2015). The area receives on average 800 mm of precipitation annually, with 60% of this total falling as snow (Hu et al., 2010). There is considerable spatial variation in precipitation throughout the catchment and temporal variation among years (Knowles et al., 2015).

The subalpine vegetation at the US-NR1 AmeriFlux site is dominated by Engelmann spruce (*Picea engelmannii*), lodgepole pine (*Pinus contorta*), and subalpine fir (*Abies lasiocarpa*) (Burns et al., 2015). Past studies have characterized the forest in the area surrounding the US-NR1 site, reporting leaf area index (LAI) ranging between 3.8 and 4.2 m^2 m^{-2}, tree heights of 12–13 m, and a canopy gap fraction of 17% (Burns et al., 2015; Monson et al., 2010; Turnipseed et al., 2002).

The US-NR1 site includes a 26 m tall flux tower with turbulent flux measurements made at a height of 21.5 m aboveground, as well as a separate tower approximately 15 m away, where measurements are taken at 2.56 m aboveground (Figure 1). In the area there are other data collection sites, including a snow telemetry (SNOTEL) site (Niwot; site number 663), a National Oceanic and Atmospheric Administration (NOAA) U.S. Climate Reference Network (USCRN) site, and a long-term climate site (C-1) (Figure 1) (Knowles et al., 2015).

3. Methods

We used three methods to estimate or simulate the presence of snow interception in the forest surrounding the US-NR1 site based on: (a) water vapor flux measurements above and below the canopy, (b) analyzing Phenocam images, and (c) simulation with three models - Community Land Model Version 5 (CLM5.0), Noah-Multiparameterization (Noah-MP) and Hedstrom and Pomeroy (1998) (HP98) (Figure 2). Harvey (2022) provides a further description of methods beyond what is outlined below.

We initially compared all three methods to a "ground truth" of human labeled Phenocam images (Figure 2). We chose January 2019 as a period to compare the various methods because it is a winter month when precipitation

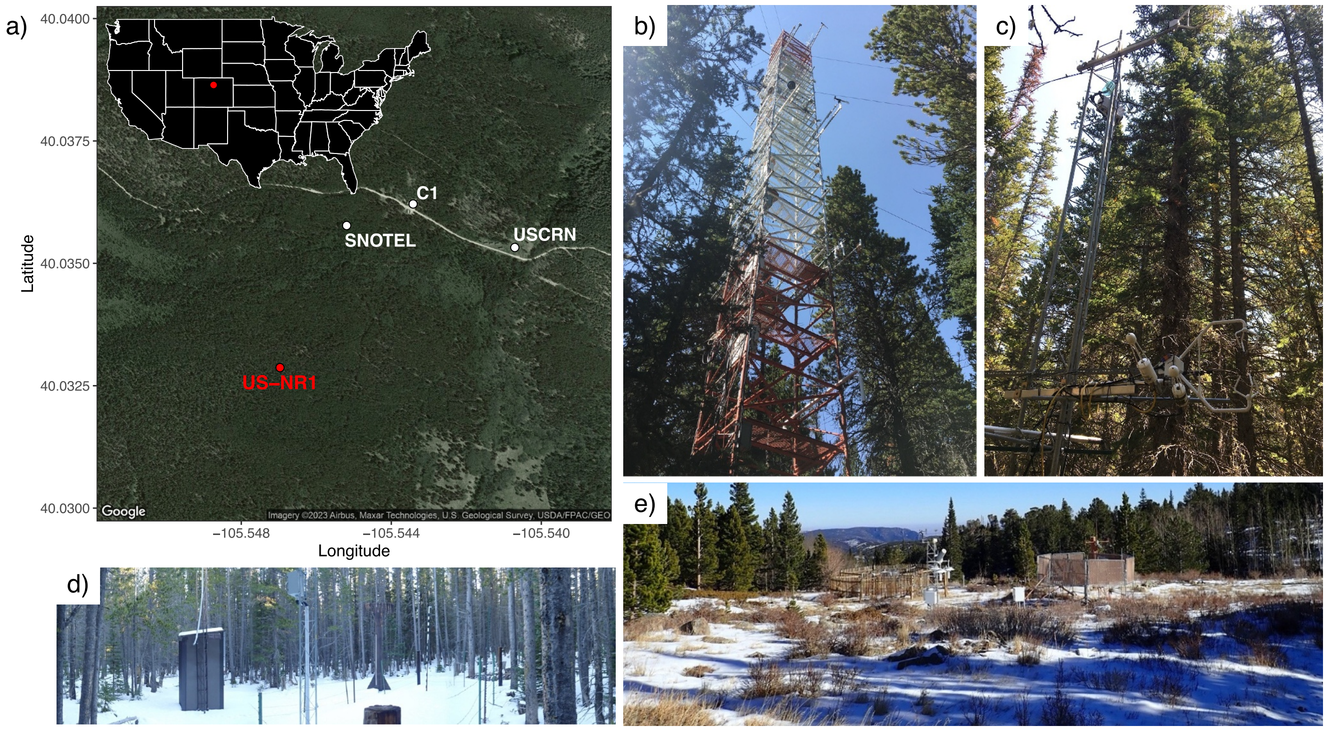

Figure 1. (a)Area around the Niwot Ridge Forest (US-NR1) AmeriFlux site, showing other data collection sites nearby including a snow telemetry (SNOTEL) site (Schaefer & Paetzold, 2001), a U.S. Climate Reference Network (USCRN) site, and a long-term climate site (C1) (Greenland, 1989) [insert shows the location of the US-NR1 site within continental United States]; (b) Niwot Ridge Forest (US-NR1) AmeriFlux site; (c) The subcanopy flux tower adjacent to the US-NR1 flux tower; (d) The snow telemetry (SNOTEL) site located in a small forest clearing near the Niwot Ridge Forest (US-NR1) AmeriFlux site; (e) The National Oceanic and Atmospheric Administration (NOAA) United States Climate Reference Network (USCRN) site located near the Niwot Ridge Forest (US-NR1) AmeriFlux site.

was likely to fall as snow, the forest was not transpiring (Bowling et al., 2018; Burns et al., 2015) and there was a continuous snowpack (Brooks et al., 1996; Burns et al., 2015). The lack of transpiration and continuous snowpack means that the water vapor flux was dominated by snow sublimation (Mahat et al., 2013; Molotch et al., 2007, 2011), with some smaller amount of snowmelt-induced evaporation. The air temperature and wind speed averages (−5.95°C and 6.23 m s^{-1} respectively) during January 2019 were comparable with long-term (1999–2018) site averages (−6.14°C and 6.83 m s^{-1}, respectively) (Figure 3). However, the mean monthly precipitation in January 2019 (85.9 mm) was 29% greater the 15-year average precipitation for the same month (66.76 mm) (Figure 3).

The most promising methods were then applied throughout the winter (1 October 2018 to 31 May 2019) (Figure 2). Due to the extensive effort and resources required, human-labeled images were not prepared as a "ground truth" for the 2018/2019 winter, preventing direct comparison and evaluation of methods using a statistical metric. Instead, we compared the methods against each other and precipitation data.

3.1. Flux Measurements

Since 1998 and 2002 respectively, above- and below-canopy latent heat flux, and other measurements, were made from a main and subcanopy tower at the US-NR1 site (Blanken et al., 2009; Burns et al., 2016; Molotch et al., 2007). Subcanopy eddy covariance instruments measured the latent heat flux at a height of 2.56 m on a smaller triangular tower approximately 15 m from the main tower. Subcanopy instruments consisted of a sonic anemometer (CSAT3, Campbell Sci. Inc.) and two infrared gas analyzers (LI-7500 and LI-7500A, LI-COR Biosciences). The comparison of the 30-min mean latent heat fluxes, calculated using the two different gas analyzers, revealed close agreement ($r = 0.92$; Harvey, 2022, Figure 2.2). Therefore, we took the average of both instrument pairs to represent sublimation from the ground snowpack to obtain the most complete record possible, henceforth referred to as subcanopy sublimation. A sonic anemometer (CSAT3, Campbell Sci. Inc.) and an infrared gas analyzer (LI-7200, LI-COR Biosciences) comprised the above-canopy (21.5 m) instruments. Burns

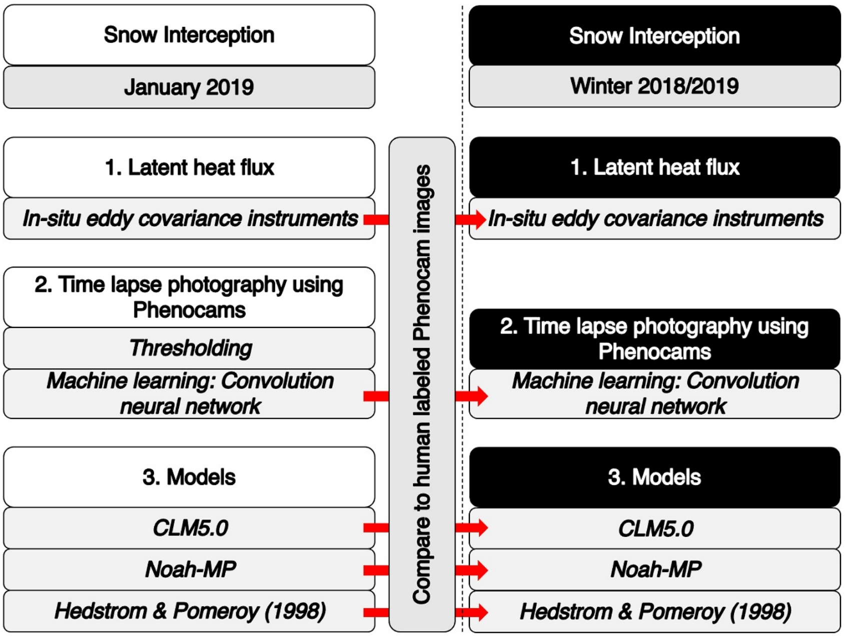

Figure 2. Overview of methodology used to compare snow interception methods. Initially several methods were used to estimate the presence of canopy snow and simulate snow interception over January 2019, with results compared to the ground truth of human labeled images. The superior methods identified during the initial phase (January 2019) were then applied to the 2018/2019 winter (CLM5.0 = Community Land Model Version 5, Noah-MP = Noah-Multiparameterization).

et al. (2014, 2016) provide further details on the instrumentation and eddy covariance data processing. We subtracted the flux measurements at the 2.56 m height from those at the 21.5 m height, assuming this difference represented the sublimation of snow intercepted on the canopy, similar to Molotch et al. (2007), Jarosz et al. (2008), and Mahat et al. (2013).

Since sublimation of intercepted snow is only possible when snow is available in the canopy, we used the two eddy covariance data sets to estimate whether sublimation of canopy snow was occurring, and therefore when snow was present in the canopy. To binarize the flux-derived interception presence, we categorized the timestep as "intercepted snow present" if the canopy water vapor flux (above-canopy minus below-canopy values) was greater than zero. We evaluated the binarized flux data using the binary evaluation metric of Balanced Accuracy Score (Equation 1) (Brodersen et al., 2010) as compared to the labeled niwot3 Phenocam images (similar to Lumbrazo et al. (2022)) due to their shared temporal resolution of 30 min.

$$\text{Balanced Accuracy} = \frac{1}{2}\left(\frac{\text{True Positive}}{\text{True Positive} + \text{False Negative}} + \frac{\text{True Negative}}{\text{True Negative} + \text{Flase Positive}}\right) \tag{1}$$

This method was then applied to the 2018/2019 winter (Figure 2). Before applying the latent heat flux method to the whole 2018/2019 winter, we ensured transpiration was not occurring. The forest around the tower commonly continues transpiring into October, becomes dormant for several months, and then starts to transpire again in April or May (Barnard et al., 2018; Bowling et al., 2018, 2024; Burns et al., 2015). While the forest is still transpiring, a positive difference between the above and below canopy flux can occur without snow on the canopy, because the above canopy measurement includes any transpiration (Burns et al., 2015). Previously, both the net ecosystem exchange of carbon dioxide (NEE) and bole temperature have been used to determine if the forest was transpiring (Bowling et al., 2018; Burns et al., 2015). Reviewing the NEE and bole temperature for the 2018/2019 winter revealed that transpiration stopped around the first of November 2018 and restarted around the fifteenth of April 2019 (Figure 4). Therefore, we applied the same latent heat flux analysis to this shortened winter period to ensure that we avoided including transpiration in the latent heat flux measurements.

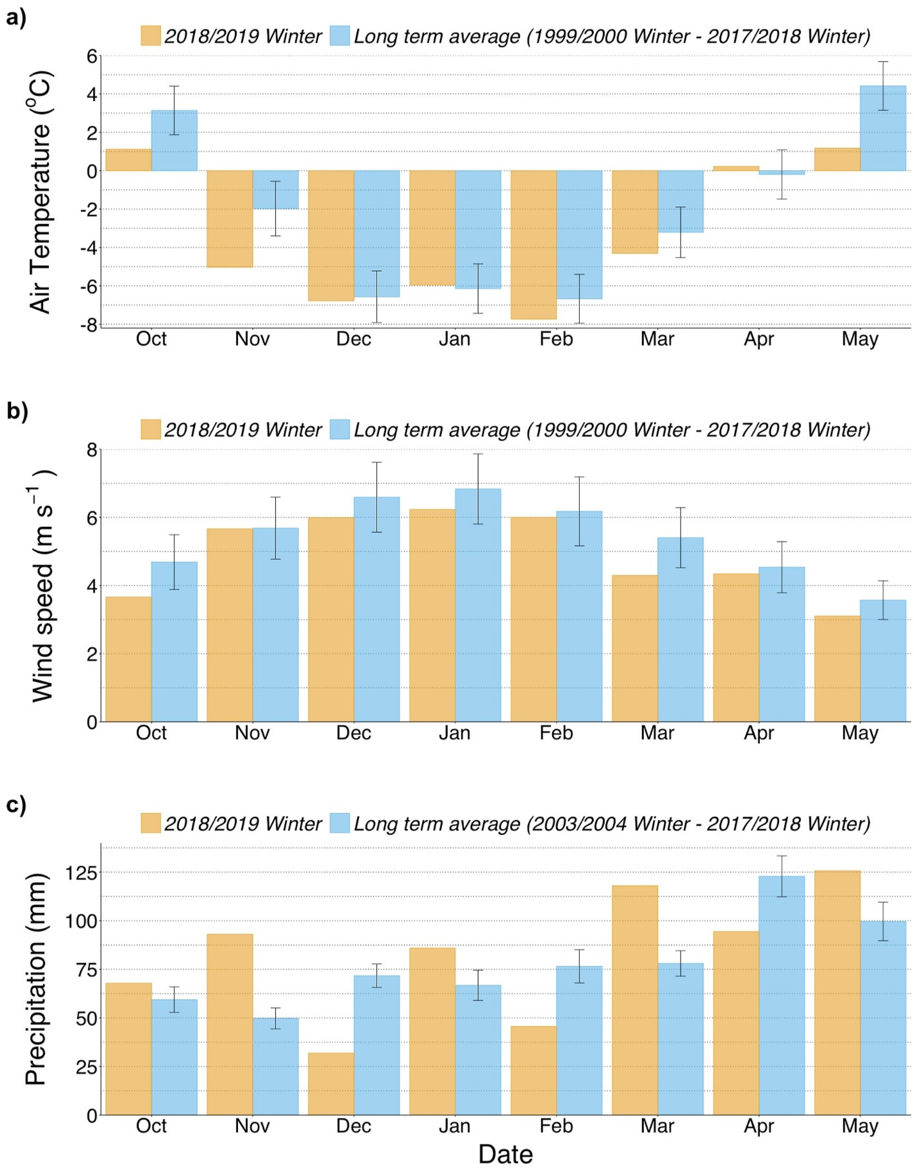

Figure 3. (a) Air temperature (°C), (b) wind speed (m s^{-1}), and (c) precipitation (mm) for the winter months (October–May), showing both the long-term average (and standard error) and 2018/2019 winter values. The air temperature and wind speed data are from the US-NR1 AmeriFlux data set and measured at 21.5 m above the ground (Figure 1). Precipitation data are from the USCRN site (Figure 1).

3.2. Phenocam Images and Processing

We used the two Phenocams (Richardson et al., 2018; Seyednasrollah et al., 2019) currently operating and mounted to the US-NR1 AmeriFlux tower (niwot3 and niwot5) to assess how images could be employed to identify snow interception using automated methods. Both cameras produce Red, Green, and Blue (RGB) images with a pixel resolution of 1,296 × 960 (Burns et al., 2016) and 8-bit radiometric resolution. The temporal resolution of niwot3 is 30-min intervals between 04:00 and 22:30 Mountain Standard Time (MST), and the temporal resolution of niwot5 is 15-min intervals between 04:00 and 22:45 MST. The niwot3 Phenocam is orientated north, while niwot5 is orientated southeast. To ensure enough light was available and the images would not be affected by sunrise or sunset, we only used images between 9:00 and 14:00 MST.

We tested two different image analysis methods: thresholding and machine learning using Convolutional Neural Networks (CNN). Before performing either method, we cropped the images (1,296 × 760 and 1,243 × 674 for

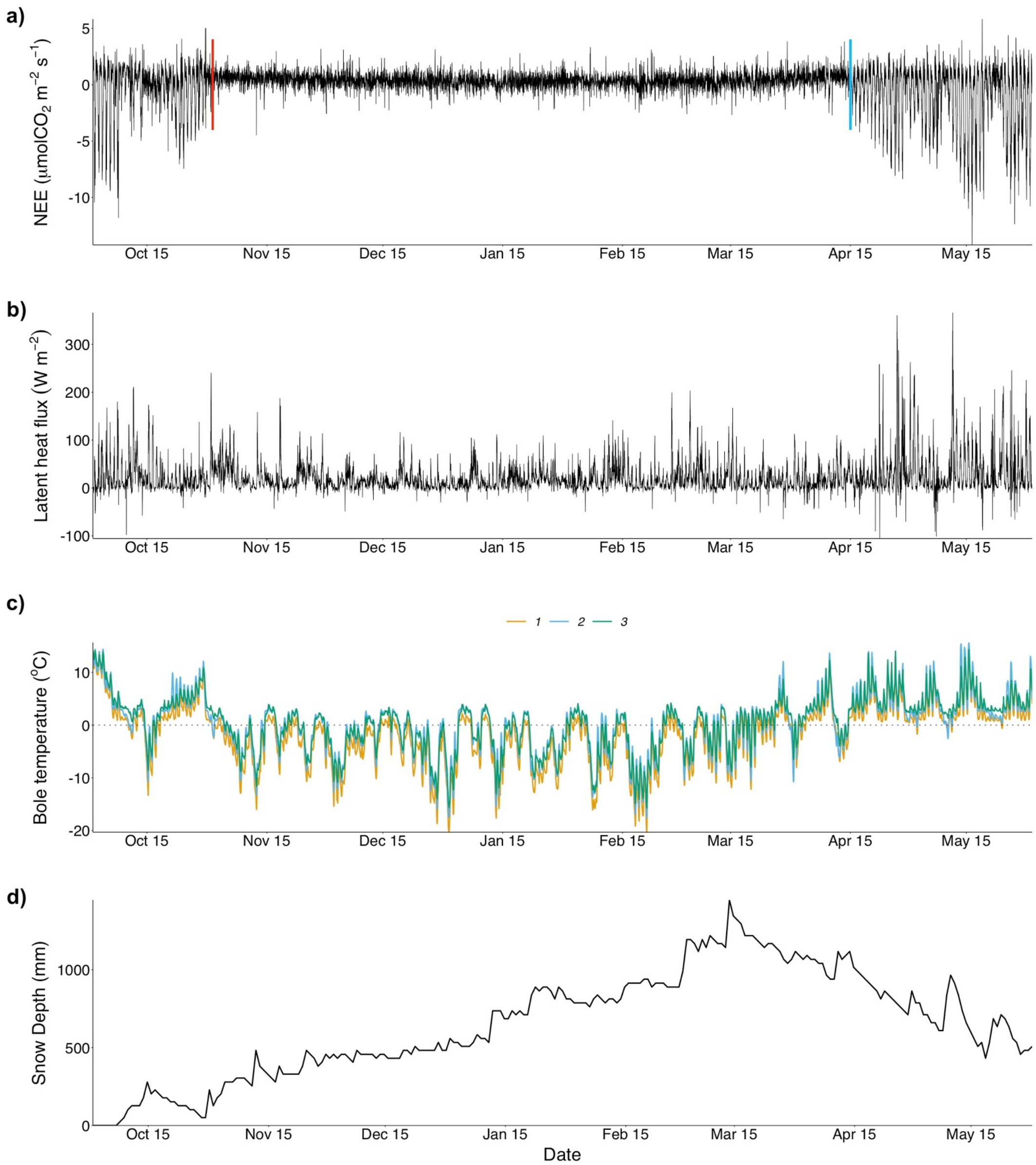

Figure 4. (a) Net ecosystem exchange (NEE) ($\mu molCO_2\ m^{-2}\ s^{-1}$), (b) above-canopy latent heat turbulent flux ($W\ m^{-2}$), (c) bole temperatures (°C), and (d) snow depth (mm) for the 2018/2019 winter (October–May inclusive). The NEE, latent heat flux, and bole temperature data ((1) lodgepole pine (*Pinus contorta*); (2) subalpine fir (*Abies lasiocarpa*); (3) Engelmann spruce (*Picea engelmannii*)) are from the Niwot Ridge Forest (US-NR1) AmeriFlux data set. The snow depth data is from the nearby Niwot SNOTEL site (site number: 663) (Figure 1). The red and blue lines on the NEE plot define when the forest was likely not transpiring.

niwot3 and niwot5, respectively) to exclude any background and image identification details, ensuring only the canopy was analyzed.

RGB images are made up of three bands - red, green, and blue - each representing a specific range of wavelengths. By isolating a single band, an RGB image becomes a grayscale image, where the digital number (DN) represents the brightness level of the pixel (e.g., with a range of 0–255 for an image with 8-bit radiometric resolution). To enable thresholding, we first isolated the blue band (Band 3), resulting in one greyscale image. We chose the blue band based on this band having the most favorable DN histograms for threshold analysis (i.e., the greatest contrast between snow and non-snow pixels). DN histograms also assisted in the setting of the threshold for differentiation between snow and non-snow. We defined snow as DN values between 220 and 253, with lower values defined as

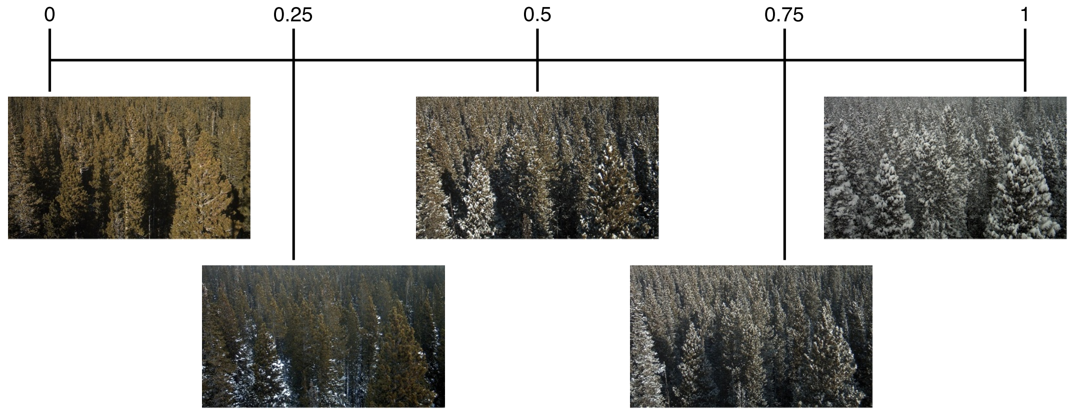

Figure 5. Visualization of the categories used when labeling the niwot3 Phenocam images. Cropped images are shown.

non-snow. We excluded DN values 254 and 255 to avoid the spike in DN values when no snow was present, which would have translated to false positives if included. Finally, we calculated the fraction of intercepted snow (%) by dividing the number of pixels classified as intercepted snow by the total number of pixels in the (cropped) image, similar to the snow interception index of Dong and Menzel (2017). We undertook thresholding analysis in MATLAB (R2021b) using the Image Processing Toolbox Version 11.3.

To allow for comparison to the "ground truth" human labeled images, we binarized the fraction of intercepted snow as calculated during thresholding. To reduce false positives, we deemed the image to include intercepted snow only if the fraction of intercepted snow was above 1% (i.e., over 1% of the pixels were classified as snow). We then evaluated the thresholding method using the Balanced Accuracy Score (Equation 1) (Brodersen et al., 2010) similar to Lumbrazo et al. (2022).

We developed, trained, and tested three CNNs. For definitions of CNN terms see Table S1 in Supporting Information S1. To the best of our knowledge this is the first time a CNN has been used to identify the presence of canopy snow from time-lapse imagery. All steps, except image labeling, took place in Python 3.7.9 using the TensorFlow Keras open-source library. A single user in a single sitting visually examined and classified all Phenocam images available for January 2019 between 09:00 and 14:00 MST from niwot3 (298 images) and niwot5 (568 images), assigning a 1 for images with snow interception and a 0 for those without. In addition to the binary labeling, we categorically labeled the images from niwot3 in 0.25 intervals from 0 to 1, where 0 was no visible snow, and 1 was maximum canopy snow loading (Figure 5). We randomly reordered the images to minimize the effect of the original order on results. We split the data into 80% for training/validation and 20% for testing, then further divided the training/validation data set into 80% for training and 20% for validation.

First, we built the CNN model architecture. The convolutional layers comprised convolutional filters (and associated activation function) and then a pooling layer. Filtering layers contained either 5 or 10 individual convolutional filters, each with a size of 3×3 and stride of 1. No padding was used when applying the convolutional filters. We used the rectified linear unit (ReLU) activation function (Han et al., 2020) during convolutional filtering. The pooling layers used Max Pooling (Wang et al., 2017). Here, we set the pooling window size and stride to 2. Figure 6 illustrates the first convolutional filtering on the input data and first pooling. We completed the model with a fully connected layer followed by a SoftMax classification layer, as the purpose of the CNN was binary or categorical classification.

We trained the model using the Adam optimizer (Han et al., 2020) with a learning rate of 0.0001. During training, we minimized the loss function binary cross-entropy for the binary classifiers and categorical cross-entropy for the categorical classifier. We used 20 epochs and a batch size of 2 for all CNN models. The model with the highest validation accuracy continued to be trained in the next epoch or became the final model when all epochs were completed. Finally, we calculated the model's Balanced Accuracy Score (Equation 1), similar to Lumbrazo et al. (2022), by comparing the model-predicted labels of the unseen test images to the human-assigned labels.

When applying image analysis to the entire 2018/2019 winter we focused on the niwot3 Phenocam because it has matching temporal resolution to the flux data and meteorological data used to force the models (30 min). We used

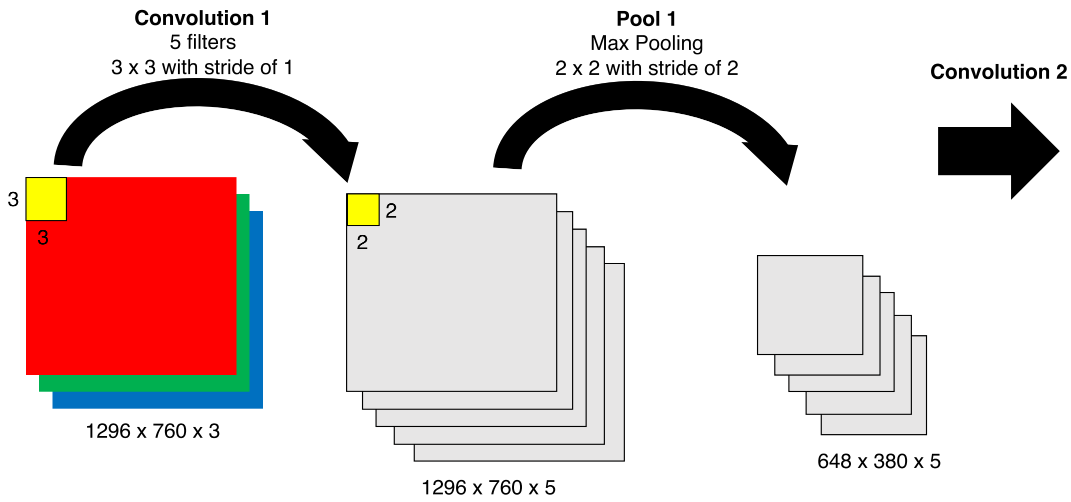

Figure 6. The first convolutional filtering and pooling for the CNN model based on a cropped niwot3 image.

the best performing CNN model during training/validation based on validation accuracy (i.e., the final model), to predict the label (snow or no snow) of unseen images throughout the rest of the 2018/2019 winter (October, November, December, February, March, April, May). To ensure daylight and consistency, we again only used images captured between 9 a.m. and 2 p.m. MST.

3.3. Snow Interception Models

We used three models of varying levels of complexity to simulate canopy snow processes (i.e., snow interception, unloading, sublimation) over January 2019 (Table 1). We ran all models with a 1-week start-up period to account for prior storms; however, we only show results from January 2019. For detailed model description see Text S1 in Supporting Information S1. To binarize the model output, we categorized the timestep as "intercepted snow present" if the model simulated canopy snow was above 0.5 kg m^{-2} (Lundquist et al., 2021). Converting the model simulations to a binary result allowed us to directly compare them to the labeled images and calculate the Balanced Accuracy Score (Equation 1) and estimate the number of days with canopy snow.

We isolated the canopy interception and canopy snow unloading algorithms used in the Community Land Model Version 5 (CLM5.0) to simulate canopy snow. CLM5.0 partitions precipitation into solid or liquid states using a linear air temperature ramp where precipitation is snow below 0°C and rain above 2°C (Lawrence et al., 2019). To align with the parameterization used for the Noah-MP model (Niu et al., 2011), we used a 0°C air temperature threshold below which precipitation is solid. We halved the published values of the leaf area index (LAI) for the forest surrounding the Niwot AmeriFlux site to represent the one-sided exposed leaf and stem area index (Turnipseed et al., 2002).

We evaluated the use of both a constant and variable sublimation rate of canopy intercepted snow in the CLM 5.0 model. In the constant sublimation rate approach, we used the average sublimation rate of intercepted snow reported by Molotch et al. (2007) for the winter/spring snow season (0.70 mm day^{-1}). In the variable sublimation rate approach, we used the difference between the above- and below-canopy water vapor flux measurements to represent the time-varying sublimation loss rates from intercepted snow. To convert the latent heat flux measurements from W m^{-2} to mm per timestep (30-min) we used a varying latent heat of evaporation (J kg^{-1}) based on the equation (Bolton, 1980). This conversion was used rather than the latent heat of sublimation (2834 kJ kg^{-1}) as the temperature dependent latent heat of evaporation is used year-round when processing data at the site so should be used when performing further conversions. This is unlike how sublimation from vegetative surfaces is calculated in the CLM5.0 model (Lawrence et al., 2020), however, here the focus is on interception dynamics rather than modeling sublimation.

The Hedstrom and Pomeroy (1998) model (HP98) calculates snow interception based on canopy characteristics and snowfall. Unloading of intercepted snow is modeled as an exponential function of time (Hedstrom & Pomeroy, 1998). Constants for the dimensionless unloading coefficient and maximum ratio of snow to leaf

Table 1
Outline of the Three Interception Models, Including a Brief Description of How Interception is Modeled, How Unloading and Other Losses of Intercepted Snow is Incorporated, and Required Input Data to Model Interception

Model name	Description of interception	Description of unloading	Required input data	Source
Community Land Model Version 5.0 (CLM5.0)	Interception is a function of precipitation and fraction of the canopy that can collect precipitation.	Unloading of snow from the canopy is driven by both air temperature and wind speed. Sublimation losses of interception snow are also included.	- Air temperature - Precipitation - Wind speed - LAI	Lawrence et al. (2019); TechnicalNote
Hedstrom and Pomeroy interception model (HP98)	Interception is a function of canopy snow load and canopy density.	Unloading of snow from the canopy is based on time since snowfall.	- Air temperature - Precipitation - LAI	Hedstrom and Pomeroy (1998)
Noah-Multiparameterization (Noah-MP)	Interception is a function of snowfall rate and the remaining storage capacity of the canopy.	Unloading of snow from the canopy is driven by both air temperature and wind speed. Sublimation losses of intercepted snow are also included.	- Air temperature - Canopy temperature - Precipitation - Wind speed - LAI	Niu et al. (2011); Niu and Yang (2004); Noah-MPCommunityModelRepository

Note. For detailed model description see Text S1 in Supporting Information S1 (LAI = leaf area index).

contact area per unit area of ground were adopted based on an analysis of the above-canopy winter wind speeds. Here the species dependent maximum snow load per unit branch area was set to the average of the values suggested by Schmidt and Gluns (1991) (6.6, 5.9, and 5.1 kg m^{-2} for pine, spruce and fir, respectively) to reflect the mixed coniferous forest surrounding the tower (Turnipseed et al., 2002). We used the empirical relationship developed by Hedstrom and Pomeroy (1998) that relates fresh snow density to air temperature.

Similar to CLM5.0, relevant equations of the Noah-MP model were isolated to simulate canopy snow. Although there are several precipitation partitioning parameterizations available (Niu et al., 2011), the simplest was used: precipitation was simulated to fall as snow when air temperature was below 0°C. This approach was also implemented in our modified version of CLM5.0. We halved the published LAI values to represent effective one-sided leaf and stem area index (Turnipseed et al., 2002). The species dependent maximum snow load per unit branch area was set to 5.87 kg m^{-2} based on the average of the values suggested by Schmidt and Gluns (1991) to reflect the mixed coniferous forest surrounding the tower (Turnipseed et al., 2002). We used the altered version of the Hedstrom and Pomeroy (1998) empirical relationship between air temperature and fresh snow density present in the Noah-MP model (Niu et al., 2011). We incorporated sublimation losses of intercepted snow into Noah-MP using the same methods applied in CLM5.0.

All models were applied to the 2018/2019 winter (Figure 2). We continued to use a one-week warm-up period, however, only results from first of October 2018 to 31st of May 2019 are shown. We considered only the CLM5.0 and Noah-MP models with constant intercepted snow sublimation losses. Again, timesteps was categorized as "intercepted snow present" if the model simulated canopy snow above 0.5 kg m^{-2} (Lundquist et al., 2021). We compared these binarized model simulations to the CNN predictions.

4. Results

4.1. Flux Measurements

When comparing the binarized canopy water vapor flux data to the "ground truth" of labeled images (Figure 2), the Balanced Accuracy Score was 0.60 (Figure 7b). There were 131 false positives compared to the 104 true positives, 32 true negatives, and zero false negatives. Subtracting the water vapor flux measurements below the canopy from those above the canopy and attributing any positive difference to the sublimation of intercepted snow (Molotch et al., 2007), misrepresented this process, as it suggested snow sublimation (and therefore the presence of interception) at most 30-min timesteps, even days after snow was observed to have left the canopy (Figure 7b).

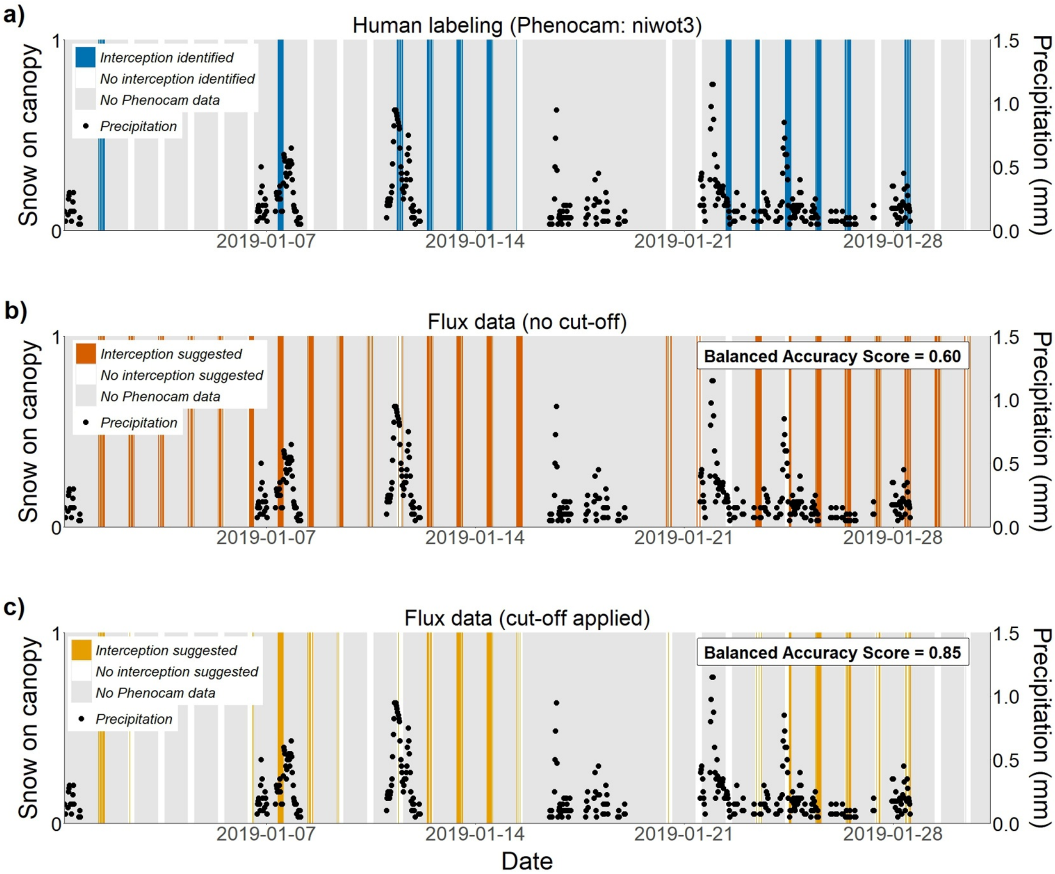

Figure 7. Binarized snow on canopy from the (a) human labeling of images from the niwot3 Phenocam, (b) flux data, and (c) flux data with cut-off. The blue bars indicate times when the images were labeled as "snow interception" by a single human observer. The red and orange bars indicate times when the binarized flux data suggested the presence of snow interception. The white bars indicate times when no interception was present, based on each method respectively. The grayed-out sections indicate when Phenocam images could not be analyzed due to light conditions (e.g., sunrise, sunset, or nighttime) or were unavailable (2019-01-16 to 2019-01-19 inclusive). The gray bars are also included in the flux data to ease with comparison; however, flux data is available at 30-min time steps both day and night. The flux data were binarized where (b) any positive difference between the above- and below-canopy measured flux was taken to indicate snow on the canopy or (c) any positive difference between the above- and below-canopy measured flux greater than 25 W m^{-2} was taken to indicate snow on the canopy. 25 W m^{-2} was the best cut-off based on the calculated Balanced Accuracy Score (Table 2). The black points indicate precipitation measured at 30-min intervals from the nearby U.S. Climate Reference Network site when air temperatures were below 0°C (Figure 1).

We tested different "cut-off" values where instead of a positive difference between above-minus below-canopy water vapor flux measurements implying sublimation, the difference had to exceed 5 W m^{-2}, 10 W m^{-2}, 15 W m^{-2} and so on until the Balanced Accuracy Score stopped improving. The highest Balanced Accuracy Score was achieved using a cut-off of 25 W m^{-2} (Balanced Accuracy Score = 0.85; Table 2; Figure 7c) and substantially reduced the number of false positives from 131 to 17. Moreover, there were 85 true positives, 146 true negatives and 21 false negatives when using the 25 W m^{-2} cut-off, increasing the number of true results from 136 to 229.

To minimize the risk of misclassifying transpiration as the sublimation of intercepted snow, we limited the application of the flux method (with cut-off) during the 2018/2019 winter (Figure 4) (Barnard et al., 2018; Bowling et al., 2018; Burns et al., 2015). During this shortened winter season, the latent heat flux method suggested the presence of canopy snow on 127 out of the 166 days (77%). Generally, the binarized results indicate that positive differences between the above and below canopy fluxes greater than 25 W m^{-2} aligned with precipitation events (Figure 8).

Table 2
Balanced Accuracy Scores Between Human Labeled niwot3 Phenocam Images and Flux Data Using Different Cut-Offs Applied After Subtracting the Measured Below-Canopy Water Vapor Flux Measurements From the Measured Above-Canopy Water Vapor Flux Measurements

Cut-off	0 W m^{-2}	5 W m^{-2}	10 W m^{-2}	15 W m^{-2}	20 W m^{-2}	25 W m^{-2}	30 W m^{-2}	35 W m^{-2}
Balanced Accuracy Score	0.60	0.71	0.80	0.82	0.83	0.85	0.83	0.79

4.2. Phenocam Images and Processing

Based on the labeling of the niwot3 Phenocam images, snow was present on the canopy for 13 of the 28 days (46%) with daytime images available. Images were unavailable from January 16th to 19 January 2019 (except for the January 16th at 9 a.m. MST) due to a network issue. On 10 of the 12 days with snow observed on the canopy (and a complete record for the day), canopy snow persisted throughout the day (9 a.m.–2 p.m. MST).

The thresholding technique demonstrated low accuracy in detecting intercepted snow when compared to the labeled data. Applied to niwot3 and niwot5 Phenocam images thresholding achieved Balanced Accuracy Scores of 0.64 and 0.68, respectively. Thresholding analysis using both the niwot3 and niwot5 images resulted in substantial false negatives, where thresholding failed to detect snow on the canopy despite human labeling indicating snow interception (Figure 9).

The Balanced Accuracy Score of the CNN models ranged from 0.96 (niwot5 binary) to 1 (niwot3 binary and niwot3 categorical) (a score of one indicates no misclassifications). Only during testing of the niwot5 binary CNN did two false positives and two false negatives occur out of 114 unseen testing images.

Based on CNN-predicted output (October 2018–May 2019, excluding January 2019) and labeled images (January 2019), snow was classified as present on the canopy for 93 out of 238 days (39%) during the winter of 2018/2019. Although the CNN was able to catch most snow interception events based on when precipitation fell, some events were missed (Figure 10). There were two periods of camera shutdown, the sixteenth to nineteenth of January and the 23rd and 24th of March (Figure 10), both of which experienced precipitation events. Such periods cannot be avoided, but likely resulted in missed interception days. Small, isolated precipitation events that occurred overnight when imagery could not be analyzed were likely also missed (Figure 10). It is therefore likely the CNN predictions underestimate the number of days with snow interception.

4.3. Snow Interception Models

The CLM and Noah-MP model was run in two different modes: constant or variable sublimation rate. The HP98 model was run in a single mode. Both versions of the CLM5.0 and Noah-MP models gave Balanced Accuracy Scores between 0.69 and 0.73 (Table 3). The HP98 model had a lower Balanced Accuracy Score of 0.50 (Table 3). However, the Balanced Accuracy Score values between the model groups were not significant based on a Kruskal-Wallis test ($H\ (2) = 2.00$, $p = 0.37$).

The number of days the models indicated intercepted snow varied between the models, from a maximum of 17 (55% of days in January 2019) to 4 (13% of days in January 2019) (Table 3). One reason behind the small number of days with simulated canopy snow when using the HP98 model was that simulated canopy snow amounts were small compared to the other models (Figure 11), so when binarizing the model data (i.e., only periods with above 0.5 kg m^{-2} were assigned as "intercepted snow present" (Lundquist et al., 2021)) small simulated interception events were excluded.

The difference between using the constant and variable values for sublimation was small due to sublimation playing a minor role in removing snow from the canopy compared to the removal from unloading (Figure 12 gives the results for CLM5.0). Unloading was dominated by wind due to the high winds during winter, coupled with low temperatures that hinder the simulation of temperature unloading (Figure 3; Harvey (2022, Figure 2.21); Turnipseed et al. (2002); Lumbrazo et al. (2022)).

The number of days with simulated canopy snow over the whole winter varied between models, from a maximum of 109 (45% of days in winter) for CLM5.0 to 94 (37% of days in winter) for Noah-MP to a minimum of 27 (11%

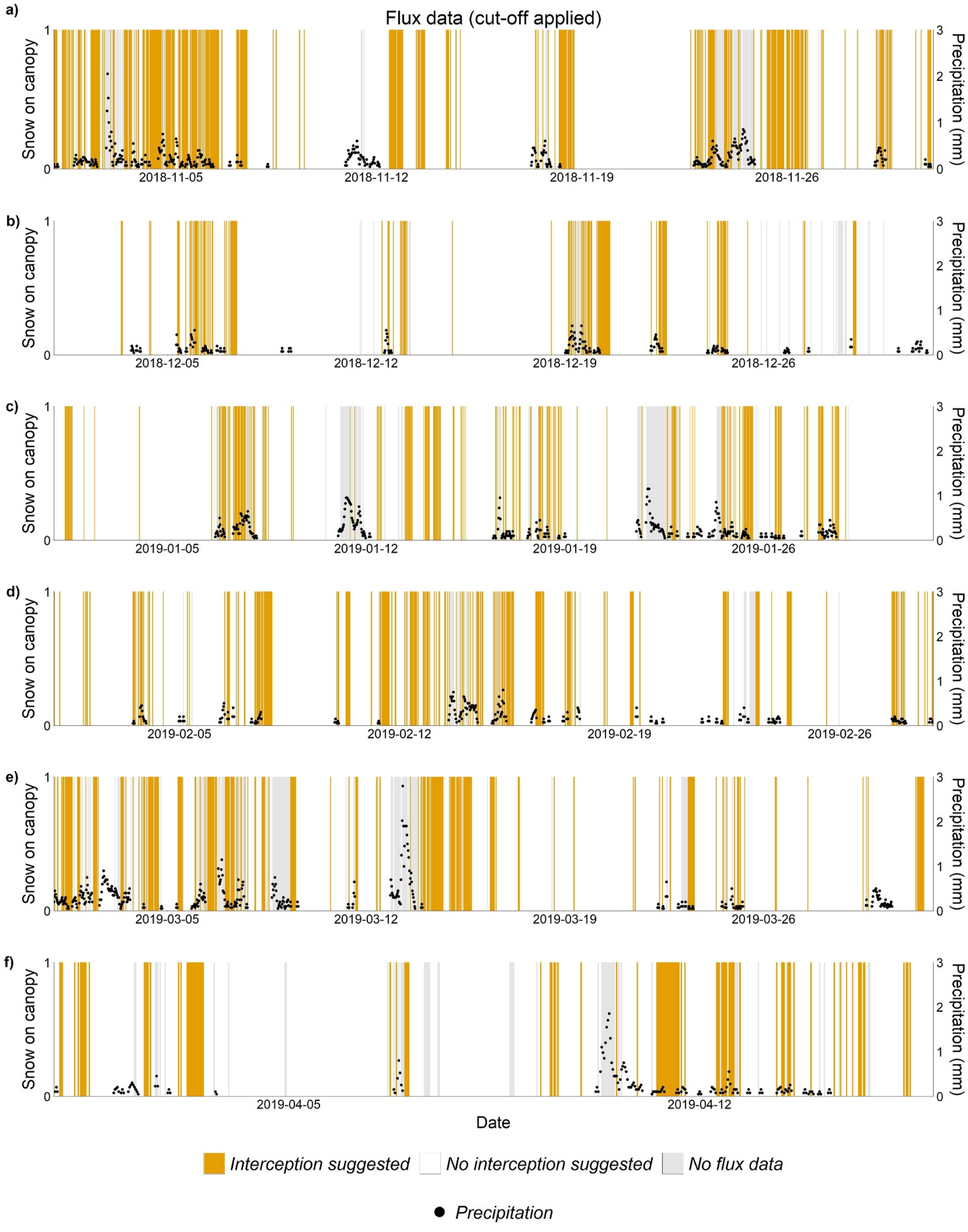

Figure 8. Binarized snow on canopy from the flux data for the 2018/2019 winter only when the forest was a dormant based on net ecosystem exchange and other factors (Figure 4)–(a) November, (b) December, (c) January, (d) February, (e) March, (f) April (until fifteenth only). The gray periods indicate when flux data were not available. The flux data was binarized where any positive difference between the above- and below-canopy measured flux greater than 25 W m^{-2} was taken to indicate snow on the canopy. 25 W m^{-2} was the best cut-off based on Balanced Accuracy Scores (Table 2). The black points indicate precipitation measured at 30-min intervals from the nearby U.S. Climate Reference Network site when air temperatures were below 0°C (Figure 1).

of days in winter) for HP98. The presence of canopy snow matched between the CNN predictions and the models 87%, 82%, and 67% of the time for CLM5.0, Noah-MP, and HP98, respectively, when both data sources were available (Figure 13).

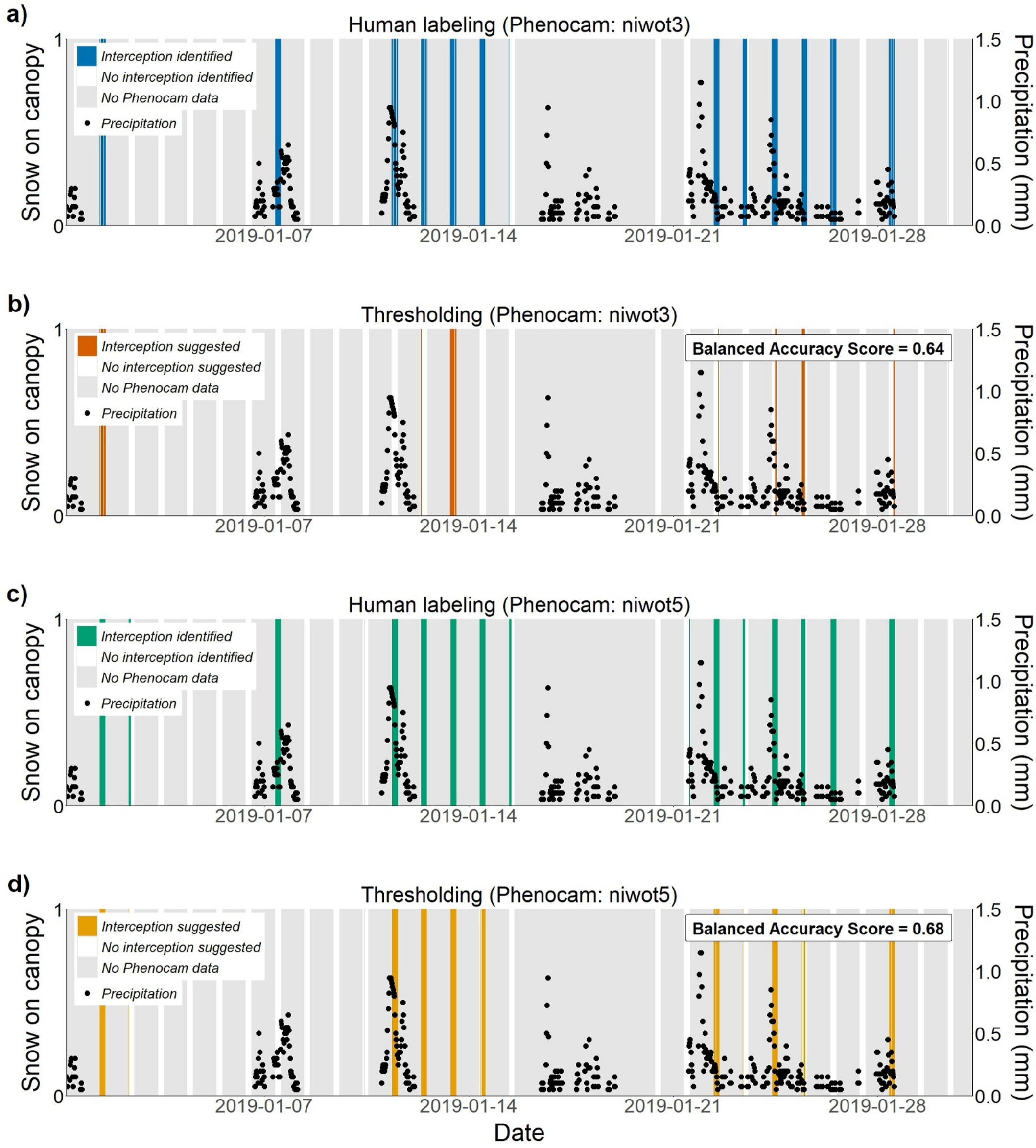

Figure 9. Binarized snow on canopy from the (a) human labeling of images from the niwot3 Phenocam, (b) thresholding method applied to the niwot3 Phenocam images, (c) human labeling of images from the niwot5 Phenocam, and (d) thresholding method applied to the niwot5 Phenocam images during January 2019. The grayed-out sections indicate times when Phenocam images could not be analyzed due to light conditions (e.g., sunrise, sunset, or nighttime) or were unavailable (2019-01-16 to 2019-01-19). The temporal resolutions of the niwot3 and niwot5 Phenocams are 30 and 15 min, respectively. The black points indicate precipitation measured at 30-min intervals from the nearby U.S. Climate Reference Network site when air temperatures were below 0°C (Figure 1).

5. Discussion

5.1. Interception in the Niwot Subalpine Over the 2018/2019 Winter

The presence of snow interception occurred between 11% and 77% of days throughout the 2018/2019 winter, based on the applied methods (Table 4). This range encompasses previously reported values, including 47% in a coniferous subalpine stand in central Switzerland (Lundberg & Halldin, 2001; Stähli et al., 2009). The CNN model predicted a low number of days with interception (39%; Table 4) as a consequence of only able to be applied during daylight hours (9 a.m.–2 p.m. MST) and therefore missing nighttime interception events

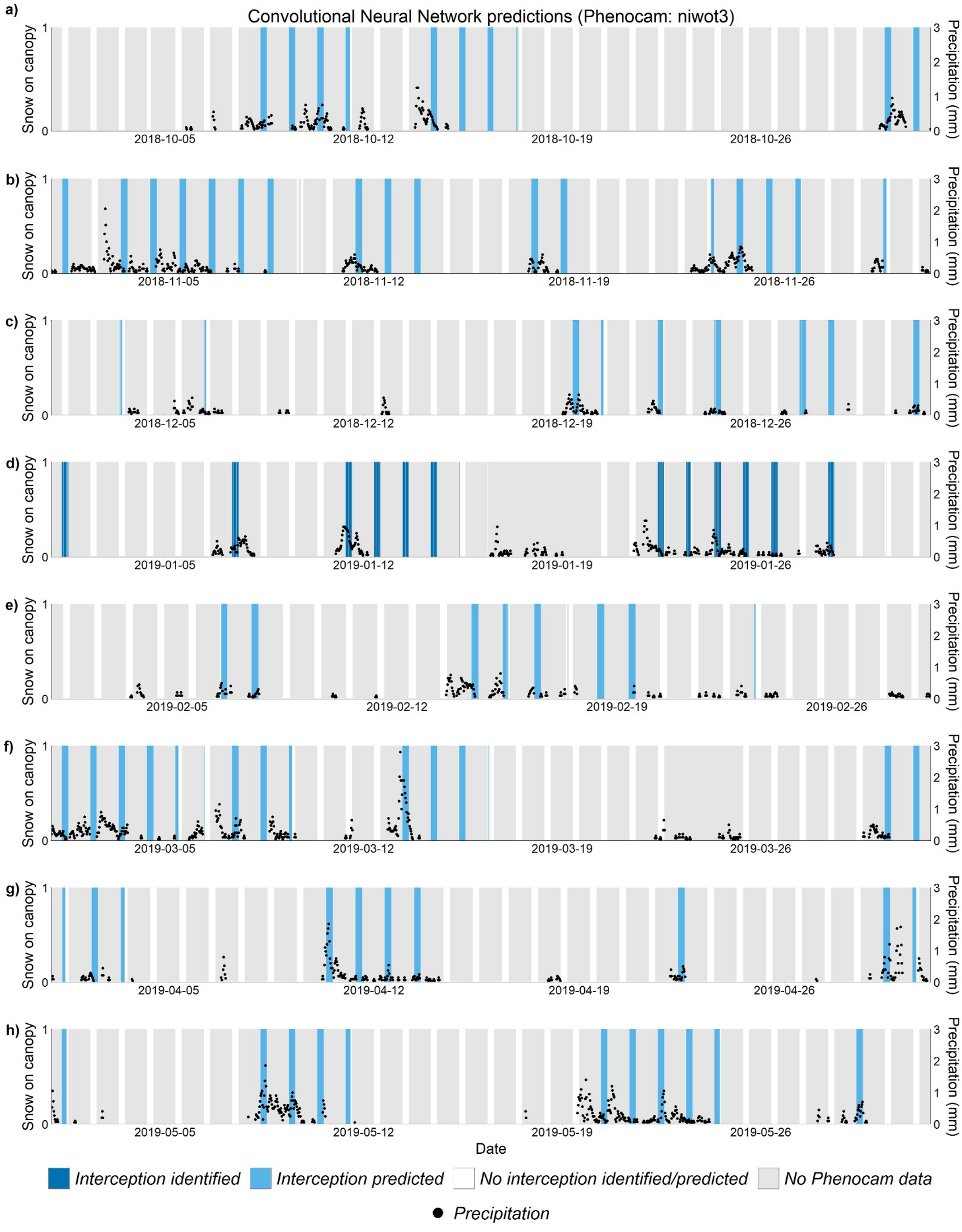

Figure 10. Snow on canopy predictions from the Convolutional Neural Network model ((a) October 2018, (b) November 2018, (c) December 2018, (e) February 2019, (f) March 2019, (g) April 2019, (h) May 2019) and human labeling ((d) January 2019) of images from the niwot3 Phenocam during the 2018/2019 winter. The gray bars indicate times when Phenocam images could not be analyzed due to poor light conditions (e.g., sunrise, sunset, or nighttime) or were unavailable. The black points indicate precipitation measured at 30-min intervals from the nearby U.S. Climate Reference Network site when air temperatures were below 0°C (Figure 1).

(Figure 10). The latent heat flux analysis predicted the most days with snow interception (77%; Table 4), even with the cut-off applied. There were times (e.g., March 15th–22nd) when the difference between the above and below latent heat flux suggested sublimation from intercepted snow for a short period bordered by periods with no difference between the measurements and without snowfall to be intercepted (Figure 8). A single period with

Table 3
Balanced Accuracy Score Scores for all Models (Simulations Binarized) Compared to Labeled Images

Model	CLM5.0 (constant sublimation)	CLM5.0 (measured sublimation)
Balanced Accuracy Score	0.73[a]	0.69[a]
Number of days with canopy snow simulated (Precent of days with canopy snow simulated)	17 (55%)	16 (52%)
Model	Noah-MP (constant sublimation)	Noah-MP (measured sublimation)
Balanced Accuracy Score	0.69[a]	0.70[a]
Number of days with canopy snow simulated (Precent of days with canopy snow simulated)	16 (52%)	14 (45%)
Model	HP98	
Balanced Accuracy Score	0.50[a]	
Number of days with canopy snow simulated (Precent of days with canopy snow simulated)	4 (13%)	

Note. Significance between model groups (i.e., CLM5.0 vs Noah-MP vs HP) are shown with superscript letters based on a Kruskal-Wallis test ($H(2) = 2.00$, $p = 0.37$). Also tabulated is the number of days with canopy snow simulated and percent (%) of days with canopy snow simulated, out of the 31 days in January 2019. Binarization used the rule: "intercepted snow present" if the model simulated canopy snow above 0.5 kg m^{-2} (Lundquist et al., 2021) (CLM5.0 = Community Land Model Version 5.0; HP98 = Hedstrom and Pomeroy interception model; Noah-MP = Noah-Multiparameterization).

above- and below-canopy latent heat flux is greater than 25 W m^{-2}, suggesting the presence of intercepted snow to be sublimated, would result in an entire day being incorrectly classified as having interception based on the methods used here. Therefore, the flux data likely overestimates the number of days with interception. The models can simulate snow interception at all timesteps (i.e., even during the night when camera imagery cannot be analyzed) and are forced by precipitation, so it is unlikely an interception event was missed. HP98 is an exception, as there were many timesteps where simulated canopy snow was below 0.5 kg m^{-2} (Figure 13), and therefore categorized as not having "intercepted snow present." Although the balanced accuracy of the models during January 2019 were less than that of the CNNs, the ability to account for interception events that occur solely during the night is a major advantage of models.

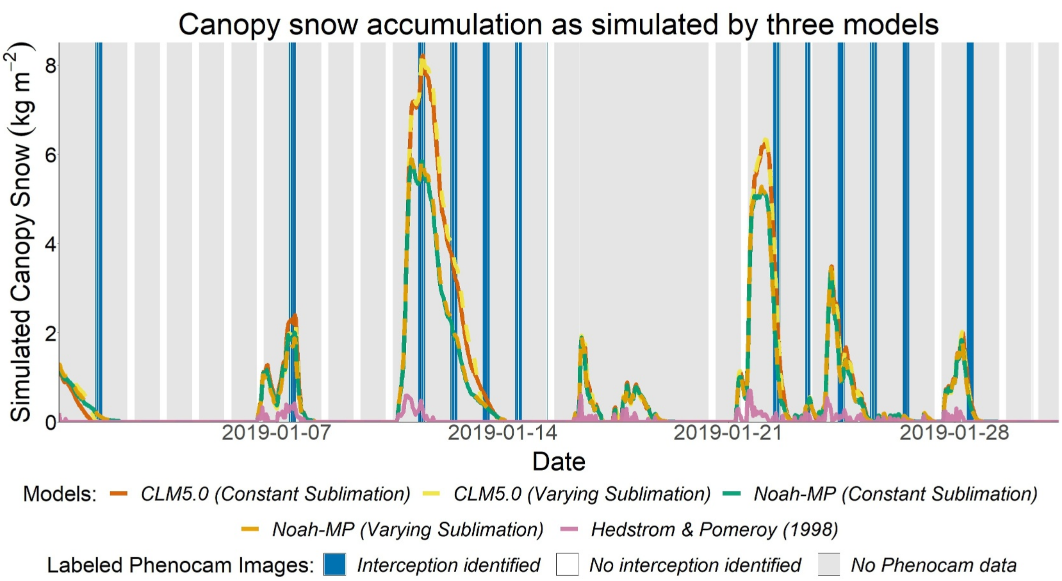

Figure 11. Time series of simulated canopy snow (kg m^{-2}) for the month of January 2019 as simulated by the simplified Community Land Model Version 5 (CLM5.0) and simplified Noah-multiparameterization (Noah-MP), using both constant sublimation losses (0.70 mm day^{-1} for the winter/spring snow season (Molotch et al., 2007)) and variable sublimation based on the difference between above- and below-canopy water vapor flux measurements, and the Hedstrom and Pomeroy (1998) interception model. The presence of snow interception, as identified by a single human observer from Phenocam (niwot3) images when available, is included as a ground truth.

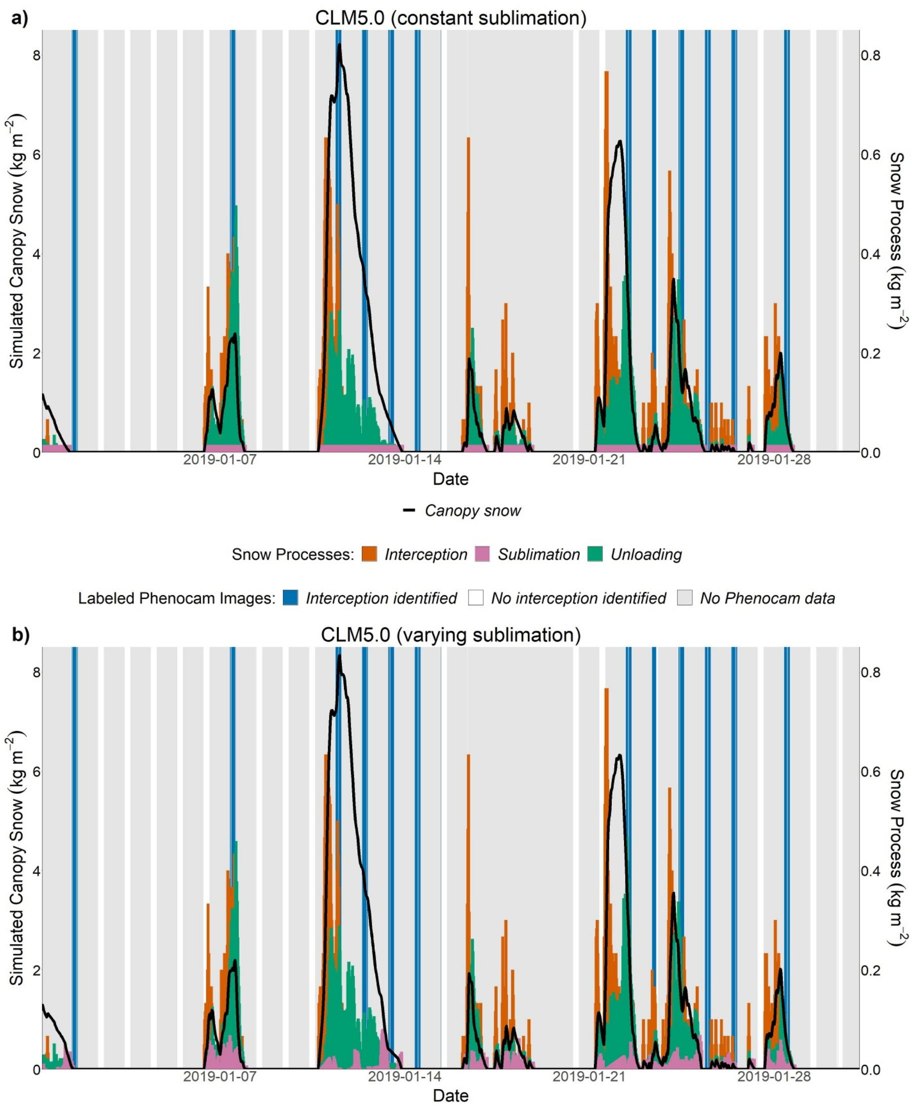

Figure 12. Time series of simulated canopy snow (kg m^{-2}) and snow process (interception, unloading, sublimation) (kg m^{-2}) for the month of January 2019 using the simplified Community Land Model Version 5 (CLM5.0). The model is run using both (a) constant sublimation based on the value reported in Molotch et al. (2007) (0.70 mm day^{-1}) and (b) variable sublimation based on the difference between above- and below-canopy water vapor flux measurements. The presence of snow interception, as identified by a single human observer from Phenocam (niwot3) images when available, is included as a ground truth.

5.2. Method Challenges and Opportunities

Two sets of eddy covariance instruments, one above the canopy and one below the canopy, have been used to measure the sublimation of intercepted snow (Mahat et al., 2013; Molotch et al., 2007). However, solely attributing the difference between above- and below-canopy water vapor flux measurements as sublimation from the forest canopy may misrepresent when snow is present in the canopy (Figure 7). One reason why a positive difference between the above- and below-canopy fluxes could occur without snow on the canopy would be the differing source areas (i.e., flux footprints) at the two measurement heights (Misson et al., 2007). Many factors dictate the flux footprint, including instrument height, turbulence, wind speed and direction, and stand characteristics (Chu et al., 2021). Therefore, the above- and below-canopy flux footprints are inherently different (Baldocchi, 1997). Another reason for a positive difference between the above- and below-canopy measures of water vapor flux without the presence of canopy snow could be the sublimation of wind-suspended snow

10.1029/2023WR036996

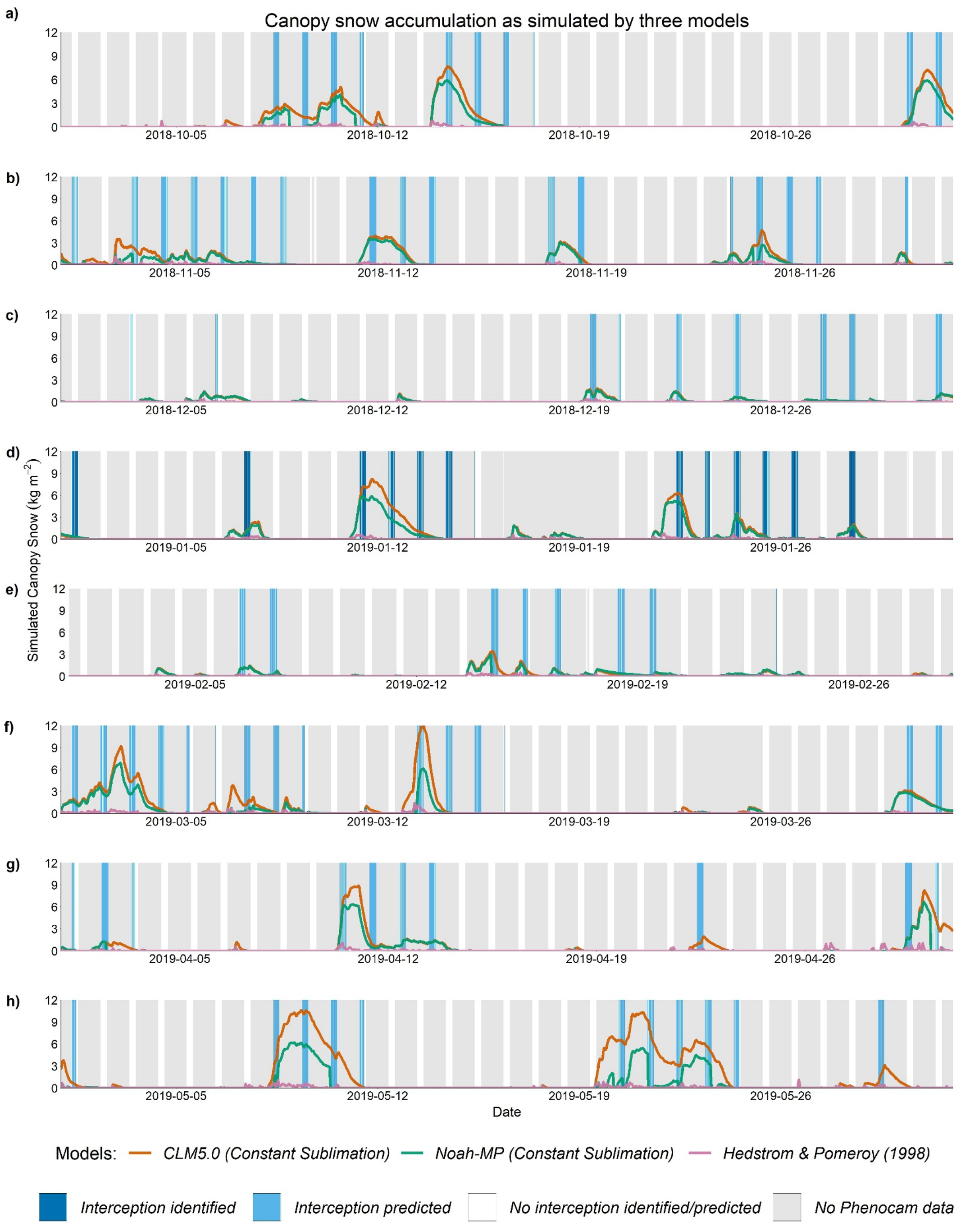

Figure 13. Time series of simulated canopy snow (kg m^{-2}) for 2018/2019 winter ((a) October 2018, (b) November 2018, (c) December 2018, (d) January 2019, (e) February 2019, (f) March 2019, (g) April 2019, (h) May 2019) as simulated by the simplified Community Land Model Version 5 (CLM5.0) and simplified Noah-multiparameterization (Noah-MP), both using constant sublimation losses (0.70 mm day^{-1} (Molotch et al., 2007)), and the Hedstrom and Pomeroy (1998) interception model. The presence of snow interception as identified by a single human observer from Phenocam (niwot3) images throughout January 2019 and predicted by the convolutional neural network model for all other months is included.

(Berg, 1986; Pomeroy & Essery, 1999; Pomeroy & Li, 2000). It is possible that the sublimation of blowing snow was measured by the eddy covariance instruments, complicating estimates of the timing and sublimation of intercepted snow using water vapor flux measurements. Accounting for the sublimation of wind-suspended snow using eddy covariance observations is difficult (Sexstone et al., 2018) and beyond the scope of this study. Additionally, there could be intercepted snow without sublimation under impeding conditions (i.e., energy

Table 4
Percent of Days With Interception (%) for all Methods Applied Over the 2018/2019 Winter

Method	Flux + cut-off + NEE constrained	CNN	CLM 5.0	Noah-MP	HP98
Percent of days with interception (%)	77	39	45	37	11

Note. The latent heat flux data used the best cut-off defined during testing (Table 2) and was constrained to ensure that transpiration was not occurring (Figure 4) (CLM5.0 = Community Land Model Version 5.0; CNN = Convolutional Neural Network; HP98 = Hedstrom and Pomeroy (1998) interception model; NEE = net ecosystem exchange; Noah-MP = Noah-Multiparameterization).

limited), further complicating the use of this method. To address these challenges practically, this study implemented a simple cut-off, which improved the Balanced Accuracy Score when comparing the flux data to the labeled images (Table 2; Figure 7) and is therefore recommended.

When applying the flux method to the entire winter, it is imperative to know when the forest stops transpiring at the start of winter, and when transpiration begins again come spring. Limiting the analysis period to when the forest was not transpiring ensures that the latent heat measurements only account for sublimation and not transpiration (Molotch et al., 2011). When forests stop and start transpiring exhibits interannual variability (Baldocchi et al., 2018; Brinkmann, 1979), meaning measurements of carbon dioxide (CO_2) turbulent fluxes are needed to determine the status of a forest. Alternatively, tree bole temperature or stem flow measurements could be used to estimate when transpiration stops and starts (Bowling et al., 2018). Without CO_2 flux or bole measurements, it would be difficult to account for sublimation for a whole winter from latent heat flux measurements, as there would be no certainty that transpiration has not been unknowingly included in the shoulder months of winter.

Time-lapse camera imagery, when used to train a CNN model, proved useful in identifying snow interception, but thresholding methods, previously successful in other studies (Floyd & Weiler, 2008; Garvelmann et al., 2013), proved difficult to apply to Phenocam images. It has been suggested to orient cameras north (in the Northern Hemisphere) to reduce direct insolation (Julitta et al., 2014; Richardson et al., 2018). However, during thresholding, images from the north-facing niwot3 Phenocam had a lower Balanced Accuracy Score (Figure 9).

When setting up cameras with the intention of applying thresholding techniques to identify interception, black, gray, and white reference boards are commonly included to enable post-processing that adjusts for varying illumination levels caused by camera contrast optimization (Floyd & Weiler, 2008; Garvelmann et al., 2013). Contrast optimization interferes during thresholding analysis, complicating the setting of fixed thresholds (Dong & Menzel, 2017). When using pre-established camera networks like the Phenocam Network, retrofitting reference boards is not possible without additional resources, if at all. Other image analysis methods, such as thresholding algorithms or deep learning, may be more suited to identifying snow interception than thresholding when reference boards are unavailable. Dong and Menzel (2017) found that the MaxEntropy thresholding algorithm, where threshold values were selected based on information content gathered from the gray levels in an image (Nichele et al., 2020; Sezgin & Sankur, 2004), was the most successful thresholding algorithm for identifying snow interception. The suitability of deep learning techniques as image analysis tools was highlighted by the improved Balanced Accuracy Score achieved by training and testing a CNN model on the labeled Phenocam images. The maximum Balanced Accuracy Score achieved during thresholding was 0.68, while a perfect Balanced Accuracy Score of one was achieved in two of the three CNN models during testing on unseen data.

We utilized a relatively small training data set compared to typical CNN applications, yet developed a highly effective tool. This tool predicts snow interception in previously unseen images and could potentially be applied to all historical and future niwot3 and niwot5 Phenocam images at US-NR1 sites. This success suggests that similar CNNs could be trained for additional sites, providing data on snow interception that might serve as a quasi "ground truth" for evaluating models, flux data, or other measurements of snow interception. Although the CNN models performed better than the thresholding technique, it is possible that the small number of data used to train the model could lead to overfitting, where the model learns data/patterns that are specific to the training set, therefore performing poorly when faced with unseen data (Yamashita et al., 2018). However, the developed models' performance during testing on unseen images was high, with Balanced Accuracy Score scores ranging from 0.96 to 1.0. To further reduce the likelihood of overfitting, additional data (i.e., images) could be used during model training (Yamashita et al., 2018). Labeling training data is resource-intensive, so other techniques could be relied on to "deform" currently labeled training data (e.g., flipping the images) to increase the training set without additional labeling (LeCun et al., 2015).

To capture and analyze images at night, it has been suggested to use near-infrared (NIR) cameras (Hedrick & Marshall, 2014). Although NIR images are available from the niwot3 Phenocam, the NIR images are produced post-processing (i.e., a NIR filter is applied to the captured RGB images), meaning that nighttime images are still unavailable. Ideally, a NIR camera would be installed, the images labeled, and a CNN built then trained. However, this approach would require additional resources and would not repurpose the extensive Phenocam Network for winter use. In contrast, the method proposed in this study requires no extra resources and adapts the existing Phenocam network for a new function: identifying canopy snow through a trained CNN. A thermal infrared (IR) camera was installed on the US-NR1 AmeriFlux tower in 2015 (Aubrecht et al., 2016). However, in the thermal IR portion of the electromagnetic spectrum the reflectance of snow is much smaller than its reflectance in the NIR portion of the electromagnetic spectrum (O'Brien & Munis, 1975; Salisbury et al., 1994). This would likely limit the usefulness of the thermal IR camera to identify snow interception.

Of the models tested, the highest Balanced Accuracy Score was achieved by the simplified CLM5.0 with a constant sublimation rate (Table 3). The addition of variable (i.e., measured flux data) sublimation data to the CLM5.0 or Noah-MP did not increase the model's performance (Table 3). This is interesting as using the calculated canopy water vapor flux data from January 2019 could not outperform a model using an average value (Molotch et al., 2007). This is attributed to sublimation playing a smaller role in removing snow from the canopy than unloading (Figure 12). The lack of meteorological driven unloading mechanisms (i.e., temperature and wind) is likely the cause of the poorer performance of the Hedstrom and Pomeroy (1998) interception model (Table 3) (Lumbrazo et al., 2022).

5.3. Interception and Sublimation Under a Changing Forest and Changing Climate

Both snow interception and sublimation are influenced by stand characteristics and meteorological conditions (Montesi et al., 2004; Roesch et al., 2001; Strasser et al., 2008). It follows that changes in forest structure or regional climate would alter these snow processes (Gelfan et al., 2004; Harpold et al., 2020; Sexstone et al., 2018).

Forest disturbance or thinning leads to a decrease in interception and sublimation of canopy snow (Harpold et al., 2020; Sexstone et al., 2018). If this reduction exceeds the increase in sublimation from the ground snowpack following disturbance or thinning (Frank et al., 2019; Harpold et al., 2020; Sexstone et al., 2018), the overall result is an increase in snow accumulation and melt volumes (Gelfan et al., 2004; Harpold et al., 2017). The Niwot Ridge subalpine forest was logged in the past (pre 1930s), with selective thinning around the US-NR1 AmeriFlux site (Burns, 2018). This suggests that volumes of snow interception and the sublimation of canopy snow were less in the past and have likely increased as the forest recovered from logging and thinning, assuming no changes in climate factors. The impact of forest changes in the Niwot subalpine forest on snow accumulation and spring runoff were not analyzed here but could be investigated using the models. The canopy parameter of the models could be varied to mirror increases in LAI as the forest regrows, simulating interception changes over time.

Snow sublimation is projected to be influenced by climate change (Sexstone et al., 2018) to a greater extent than changes produced by vegetation disturbance or growth (Gelfan et al., 2004). The volume of sublimation losses will decrease in response to reductions in snowpacks, snow area and snow duration (Sexstone et al., 2018). However, sublimation losses relative to precipitation will increase (McCabe & Wolock, 2009; Sexstone et al., 2018). The sublimation of intercepted snow is particularly sensitive to temperature; however, the projected direction of change under increasing temperatures is surprising (Rasouli et al., 2014). Intercepted snow sublimation is expected to decrease under a warming climate, as temperature unloading will remove snow from the canopy more quickly, temporally limiting sublimation of canopy snow (Gelfan et al., 2004; Rasouli et al., 2014). The CLM5.0 or Noah-MP model employed here could be used to simulate unloading regimes under changing climates by varying the forcing data (e.g., temperature).

Alongside other meteorological conditions both wind speeds and vapor pressure deficit (VPD) are expected to change with a changing climate (Liu et al., 2013), possibly catalyzing modifications to current interception and sublimation regimes. Winter windspeed are projected to be consistent or slightly increase from current conditions in the region (i.e., mountains of Colorado); however, the spring wind speeds are projected to increase (Liu et al., 2013). Snow is still likely to fall in spring in the Niwot subalpine, historically associated with reduced wind speeds compared to winter (Figure 3). An increase in wind speed would result in increased wind unloading, reducing the longevity of intercepted snow. This would suggest that more snow would be unloaded, join the ground snowpack, and possibly melt. However, sublimation rates increase with increasing wind speed (Montesi et al., 2004; Strasser et al., 2008). Determining how the two competing changes of increased wind unloading to the ground snowpack and increased sublimation from both intercepted and ground snow interact is beyond the scope of this study but could be explored through modeling. VPD is projected to increase across much of continental US, particularly during spring and summer (Ficklin & Novick, 2017). Sublimation is heavily influenced by VPD (Phillips, 2013), with increasing VPD leading to increased sublimation (Stigter et al., 2018). It follows that the projected increase in VPD will likely increase sublimation losses, further reducing snowpacks.

6. Conclusion

Although the process of snow interception is important in subalpine forests (Pomeroy & Schmidt, 1993; Stähli et al., 2009; Suzuki & Nakai, 2008), it is difficult to measure at large spatial scales (Garvelmann et al., 2013). Time-lapse camera imagery has been used to understand interception beyond the tree scale and to evaluate models (Dong & Menzel, 2017; Floyd & Weiler, 2008; Lumbrazo et al., 2022; Parajka et al., 2012). We compared different methods to identify snow interception at the US-NR1 AmeriFlux site in Colorado over January 2019. The best performing method was the Convolutional Neural Network (CNN) trained on imagery from the available Phenocams. Select methods were applied to the 2018/2019 winter. Intercepted snow was detected on at least 11% of winter days and up to 77% of winter days, depending on the method used to assess the presence of canopy snow. Beyond the performance of the methods, data availability should be considered when deciding which method is most applicable at a site. CNNs require labeled data to train the model (LeCun et al., 2015), while models require meteorological forcing data (Liston & Elder, 2006). An additional drawback of CNNs, beyond the labor-intensive labeling of training data, is their inability to analyze nighttime RGB images, likely resulting in short overnight interception events being missed.

Data Availability Statement

Data used in this research were provided by the PhenoCam Network (Richardson et al., 2018; Seyednasrollah et al., 2019), which has been supported by the National Science Foundation, the Long-Term Agroecosystem Research (LTAR) network which is supported by the United States Department of Agriculture (USDA), the U.S. Department of Energy, the U.S. Geological Survey, the Northeastern States Research Cooperative, and the USA National Phenology Network. We thank the PhenoCam Network collaborators, including site PIs and technicians, for publicly sharing the data that were used in this paper. AmeriFlux data for the US-NR1 Niwot Ridge Forest site is available from Blanken et al. (2024). Subcanopy data are available by request to the tower team of the US-NR1 AmeriFlux site (Blanken et al., 2024).

Acknowledgments
N. Harvey would like to thank Nayoung Hur and Behzad Vahedi, who both assisted in setting up the machine learning portion of this work. Funding for the US-NR1 AmeriFlux Core Site was provided by the AmeriFlux Management Project Grant number 7542010. We also thank the Phenocam Network for providing images, as well as the USCRN site for providing precipitation data. Many thanks to the three anonymous reviewers and Associate Editor for their constructive feedback on the manuscript. Open access publishing facilitated by Australian National University, as part of the Wiley - Australian National University agreement via the Council of Australian University Librarians.

References

Adam, J. C., Hamlet, A. F., & Lettenmaier, D. P. (2009). Implications of global climate change for snowmelt hydrology in the twenty-first century. *Hydrological Processes*, *23*(7), 962–972. https://doi.org/10.1002/hyp.7201

Andreadis, K. M., Storck, P., & Lettenmaier, D. P. (2009). Modeling snow accumulation and ablation processes in forested environments. *Water Resources Research*, *45*(5). https://doi.org/10.1029/2008wr007042

Aubrecht, D. M., Helliker, B. R., Goulden, M. L., Roberts, D. A., Still, C. J., & Richardson, A. D. (2016). Continuous, long-term, high-frequency thermal imaging of vegetation: Uncertainties and recommended best practices. *Agricultural and Forest Meteorology*, *228–229*, 315–326. https://doi.org/10.1016/j.agrformet.2016.07.017

Baldocchi, D. (1997). Flux footprints within and over forest canopies. *Boundary-Layer Meteorology*, *85*(2), 273–292. https://doi.org/10.1023/A:1000472717236

Baldocchi, D., Chu, H., & Reichstein, M. (2018). Inter-annual variability of net and gross ecosystem carbon fluxes: A review. *Agricultural and Forest Meteorology*, *249*, 520–533. https://doi.org/10.1016/j.agrformet.2017.05.015

Barnard, D. M., Knowles, J. F., Barnard, H. R., Goulden, M. L., Hu, J., Litvak, M. E., & Molotch, N. P. (2018). Reevaluating growing season length controls on net ecosystem production in evergreen conifer forests. *Scientific Reports*, *8*(1), 17973. https://doi.org/10.1038/s41598-018-36065-0

Bartlett, P. A., & Verseghy, D. L. (2015). Modified treatment of intercepted snow improves the simulated forest albedo in the Canadian Land Surface Scheme. *Hydrological Processes*, *29*(14), 3208–3226. https://doi.org/10.1002/hyp.10431

Berg, N. H. (1986). Blowing snow at a Colorado alpine site: Measurements and implications. *Arctic and Alpine Research*, *18*(2), 147–161. https://doi.org/10.2307/1551124

Beven, K. (2005). *Rainfall-runoff modelling: The primer* (2nd ed.). Lancaster University, UK: Wiley-Blackwell.

Blanken, P. D., Monson, R. K., Burns, S. P., Bowling, D. R., & Turnipseed, A. A. (2024). AmeriFlux BASE US-NR1 Niwot Ridge Forest (LTER NWT1) (version 21-5) [Dataset]. *AmeriFlux AMP*. https://doi.org/10.17190/AMF/1246088

Blanken, P. D., Williams, M. W., Burns, S. P., Monson, R. K., Knowles, J., Chowanski, K., & Ackerman, T. (2009). A comparison of water and carbon dioxide exchange at a windy alpine tundra and subalpine forest site near Niwot Ridge, Colorado. *Biogeochemistry*, *95*(1), 61–76. https://doi.org/10.1007/s10533-009-9325-9

Bolton, D. (1980). The computation of equivalent potential temperature. *Monthly Weather Review*, *108*(7), 1046–1053. https://doi.org/10.1175/1520-0493(1980)108<1046:TCOEPT>2.0.CO;2

Bowling, D. R., Logan, B. A., Hufkens, K., Aubrecht, D. M., Richardson, A. D., Burns, S. P., et al. (2018). Limitations to winter and spring photosynthesis of a Rocky Mountain subalpine forest. *Agricultural and Forest Meteorology*, *252*, 241–255. https://doi.org/10.1016/j.agrformet.2018.01.025

Bowling, D. R., Schädel, C., Smith, K. R., Richardson, A. D., Bahn, M., Arain, M. A., et al. (2024). Phenology of photosynthesis in winter-dormant temperate and boreal forests: Long-term observations from flux towers and quantitative evaluation of phenology models. *Journal of Geophysical Research: Biogeosciences*, *129*(5), e2023JG007839. https://doi.org/10.1029/2023JG007839

Brinkmann, W. A. R. (1979). Growing season length as an indicator of climatic variations? *Climatic Change*, *2*(2), 127–138. https://doi.org/10.1007/BF00133219

Brodersen, K. H., Ong, C. S., Stephan, K. E., & Buhmann, J. M. (2010). The balanced accuracy and its posterior distribution. In *2010 20th International Conference on Pattern Recognition* (pp. 3121–3124). https://doi.org/10.1109/ICPR.2010.764

Brooks, P. D., Williams, M. W., & Schmidt, S. K. (1996). Microbial activity under alpine snowpacks, Niwot Ridge, Colorado. *Biogeochemistry*, *32*(2), 93–113. https://doi.org/10.1007/BF00000354

Burns, S. P. (2018). *The influence of warm-season precipitation on water cycling and the surface energy budget within and just-above a Colorado subalpine forest in mountainous terrain: Measurements and modeling*. (PhD Thesis). University of Colorado at Boulder.

Burns, S. P., Blanken, P. D., Turnipseed, A. A., Hu, J., & Monson, R. K. (2015). The influence of warm-season precipitation on the diel cycle of the surface energy balance and carbon dioxide at a Colorado subalpine forest site. *Biogeosciences*, *12*(23), 7349–7377. https://doi.org/10.5194/bg-12-7349-2015

Burns, S. P., Maclean, G. D., Blanken, P. D., Oncley, S. P., Semmer, S. R., & Monson, R. K. (2016). The niwot Ridge Subalpine forest US-NR1 AmeriFlux site - Part 1: Data acquisition and site record keeping. *Geoscientific Instrumentation, Methods and Data Systems*, *5*(2), 451–471. https://doi.org/10.5194/gi-5-451-2016

Burns, S. P., Molotch, N. P., Williams, M. W., Knowles, J. F., Seok, B., Monson, R. K., et al. (2014). Snow temperature changes within a seasonal snowpack and their relationship to turbulent fluxes of sensible and latent heat. *Journal of Hydrometeorology*, *15*(1), 117–142. https://doi.org/10.1175/jhm-d-13-026.1

Chu, H., Luo, X., Ouyang, Z., Chan, W. S., Dengel, S., Biraud, S. C., et al. (2021). Representativeness of Eddy-Covariance flux footprints for areas surrounding AmeriFlux sites. *Agricultural and Forest Meteorology*, *301*, 108350. https://doi.org/10.1016/j.agrformet.2021.108350

Dong, C., & Menzel, L. (2017). Snow process monitoring in montane forests with time-lapse photography. *Hydrological Processes*, *31*(16), 2872–2886. https://doi.org/10.1002/hyp.11229

Ficklin, D. L., & Novick, K. A. (2017). Historic and projected changes in vapor pressure deficit suggest a continental-scale drying of the United States atmosphere. *Journal of Geophysical Research: Atmospheres*, *122*(4), 2061–2079. https://doi.org/10.1002/2016JD025855

Floyd, W., & Weiler, M. (2008). Measuring snow accumulation and ablation dynamics during rain-on-snow events: Innovative measurement techniques. *Hydrological Processes: International Journal*, *22*(24), 4805–4812. https://doi.org/10.1002/hyp.7142

Frank, J. M., Massman, W. J., Ewers, B. E., & Williams, D. G. (2019). Bayesian analyses of 17 winters of water vapor fluxes show bark beetles reduce sublimation. *Water Resources Research*, *55*(2), 1598–1623. https://doi.org/10.1029/2018WR023054

Garvelmann, J., Pohl, S., & Weiler, M. (2013). From observation to the quantification of snow processes with a time-lapse camera network. *Hydrology and Earth System Sciences*, *17*(4), 1415–1429. https://doi.org/10.5194/hess-17-1415-2013

Gelfan, A. N., Pomeroy, J. W., & Kuchment, L. S. (2004). Modeling forest cover influences on snow accumulation, sublimation, and melt. *Journal of Hydrometeorology*, *5*(5), 785–803. https://doi.org/10.1175/1525-7541(2004)005<0785:MFCIOS>2.0.CO;2

Greenland, D. (1989). The Climate of Niwot Ridge, Front Range, Colorado, U.S.A. *Arctic and Alpine Research*, *21*(4), 380–391. https://doi.org/10.1080/00040851.1989.12002751

Gutmann, E. D. (2020). Global Modeling of Precipitation Partitioning by Vegetation and Their Applications. In I. T. Van Stan John, E. Gutmann, & J. Friesen (Eds.), *Precipitation partitioning by vegetation: A Global Synthesis* (pp. 105–120). Springer International Publishing. https://doi.org/10.1007/978-3-030-29702-2_7

Han, Y., Wei, C., Zhou, R., Hong, Z., Zhang, Y., & Yang, S. (2020). Combining 3D-CNN and Squeeze-and-Excitation Networks for Remote Sensing Sea Ice Image Classification. *Mathematical Problems in Engineering*, *2020*, 80653966–80654015. https://doi.org/10.1155/2020/8065396

Harpold, A. A., Kaplan, M. L., Klos, P. Z., Link, T., McNamara, J. P., Rajagopal, S., et al. (2017). Rain or snow: Hydrologic processes, observations, prediction, and research needs. *Hydrology and Earth System Sciences*, *21*(1), 1–22. https://doi.org/10.5194/hess-21-1-2017

Harpold, A. A., Krogh, S. A., Kohler, M., Eckberg, D., Greenberg, J., Sterle, G., & Broxton, P. D. (2020). Increasing the efficacy of forest thinning for snow using high-resolution modeling: A proof of concept in the Lake Tahoe Basin, California, USA. *Ecohydrology*, *13*(4), e2203. https://doi.org/10.1002/eco.2203

Harvey, N. (2022). *Testing and applying methods to assess snow interception at a subalpine site (M.A.)*. University of Colorado at. Retrieved from https://www.proquest.com/docview/2716918351/abstract/80BECB3FDFBB41FDPQ/1

Hedrick, A., & Marshall, H.-P. (2014). Automated Snow Depth Measurements in Avalanche Terrain Using Time-Lapse Photography. *Presented at the International Snow Science Workshop*. https://doi.org/10.13140/2.1.2049.6646

Hedstrom, N. R., & Pomeroy, J. W. (1998). Measurements and modelling of snow interception in the boreal forest. *Hydrological Processes*, *12*(10–11), 1611–1625. https://doi.org/10.1002/(sici)1099-1085(199808/09)12:10/11<1611::aid-hyp684>3.0.co;2-4

Hu, J., Moore, D. J. P., Burns, S. P., & Monson, R. K. (2010). Longer growing seasons lead to less carbon sequestration by a subalpine forest. *Global Change Biology*, *16*(2), 771–783. https://doi.org/10.1111/j.1365-2486.2009.01967.x

Jarosz, N., Brunet, Y., Lamaud, E., Irvine, M., Bonnefond, J.-M., & Loustau, D. (2008). Carbon dioxide and energy flux partitioning between the understorey and the overstorey of a maritime pine forest during a year with reduced soil water availability. *Agricultural and Forest Meteorology*, *148*(10), 1508–1523. https://doi.org/10.1016/j.agrformet.2008.05.001

Julitta, T., Cremonese, E., Migliavacca, M., Colombo, R., Galvagno, M., Siniscalco, C., et al. (2014). Using digital camera images to analyse snowmelt and phenology of a subalpine grassland. *Agricultural and Forest Meteorology*, *198–199*, 116–125. https://doi.org/10.1016/j.agrformet.2014.08.007

Knowles, J. F., Harpold, A. A., Cowie, R., Zeliff, M., Barnard, H. R., Burns, S. P., et al. (2015). The relative contributions of alpine and subalpine ecosystems to the water balance of a mountainous, headwater catchment. *Hydrological Processes*, *29*(22), 4794–4808. https://doi.org/10.1002/hyp.10526

Lawrence, D. M., Fisher, R., Koven, C., Oleson, K., Swenson, S., & Vertenstein, M. (2020). *Community land model (CLM5.0) documentation*. National Center for Atmospheric Research (NCAR). Retrieved from https://www.cesm.ucar.edu/models/cesm2/land/CLM50_Tech_Note.pdf

Lawrence, D. M., Fisher, R. A., Koven, C. D., Oleson, K. W., Swenson, S. C., Bonan, G., et al. (2019). The Community Land Model Version 5: Description of New Features, Benchmarking, and Impact of Forcing Uncertainty. *Journal of Advances in Modeling Earth Systems*, *11*(12), 4245–4287. https://doi.org/10.1029/2018ms001583

LeCun, Y., Bengio, Y., & Hinton, G. (2015). Deep learning. *Nature*, *521*(7553), 436–444. https://doi.org/10.1038/nature14539

Liston, G. E., & Elder, K. (2006). A distributed snow-evolution modeling system (SnowModel). *Journal of Hydrometeorology*, *7*(6), 1259–1276. https://doi.org/10.1175/jhm548.1

Liu, Y., Goodrick, L., & Stanturf, A. (2013). Future U.S. wildfire potential trends projected using a dynamically downscaled climate change scenario. *Forest Ecology and Management*, *294*, 120–135. https://doi.org/10.1016/j.foreco.2012.06.049

Lumbrazo, C., Bennett, A., Currier, W. R., Nijssen, B., & Lundquist, J. (2022). Evaluating Multiple Canopy-Snow Unloading Parameterizations in SUMMA With Time-Lapse Photography Characterized by Citizen Scientists. *Water Resources Research*, *58*(6), e2021WR030852. https://doi.org/10.1029/2021WR030852

Lundberg, A., & Halldin, S. (1994). Evaporation of intercepted snow: Analysis of governing factors. *Water Resources Research*, *30*(9), 2587–2598. https://doi.org/10.1029/94wr00873

Lundberg, A., & Halldin, S. (2001). Snow interception evaporation. Review of measurement techniques, processes, and models. *Theoretical and Applied Climatology*, *70*(1–4), 117–133. https://doi.org/10.1007/s007040170010

Lundquist, J. D., Dickerson-Lange, S., Gutmann, E., Jonas, T., Lumbrazo, C., & Reynolds, D. (2021). Snow interception modelling: Isolated observations have led to many land surface models lacking appropriate temperature sensitivities. *Hydrological Processes*, *35*(7), e14274. https://doi.org/10.1002/hyp.14274

Lundquist, J. D., Vano, J., Gutmann, E., Hogan, D., Schwat, E., Haugeneder, M., et al. (2024). Sublimation of Snow. *Bulletin of the American Meteorological Society*, *105*(6), E975–E990. https://doi.org/10.1175/BAMS-D-23-0191.1

Lv, Z., & Pomeroy, J. W. (2019). Detecting intercepted snow on mountain needleleaf forest canopies using satellite remote sensing. *Remote Sensing of Environment*, *231*, 111222. https://doi.org/10.1016/j.rse.2019.111222

Mahat, V., Tarboton, D. G., & Molotch, N. P. (2013). Testing above-and below-canopy representations of turbulent fluxes in an energy balance snowmelt model. *Water Resources Research*, *49*(2), 1107–1122. https://doi.org/10.1002/wrcr.20073

McCabe, G. J., & Wolock, D. M. (2009). Recent Declines in Western U.S. Snowpack in the Context of Twentieth-Century Climate Variability. *Earth Interactions*, *13*(12), 1–15. https://doi.org/10.1175/2009EI283.1

Misson, L., Baldocchi, D. D., Black, T. A., Blanken, P. D., Brunet, Y., Curiel Yuste, J., et al. (2007). Partitioning forest carbon fluxes with overstory and understory eddy-covariance measurements: A synthesis based on FLUXNET data. *Agricultural and Forest Meteorology*, *144*(1), 14–31. https://doi.org/10.1016/j.agrformet.2007.01.006

Molotch, N. P., Blanken, P. D., & Link, T. E. (2011). Snow: Hydrological and ecological feedbacks in forests. In *Forest Hydrology and Biogeochemistry* (pp. 541–555). Springer.

Molotch, N. P., Blanken, P. D., Williams, M. W., Turnipseed, A. A., Monson, R. K., & Margulis, S. A. (2007). Estimating sublimation of intercepted and sub-canopy snow using eddy covariance systems. *Hydrological Processes: International Journal*, *21*(12), 1567–1575. https://doi.org/10.1002/hyp.6719

Monson, R. K., Prater, M. R., Hu, J., Burns, S. P., Sparks, J. P., Sparks, K. L., & Scott-Denton, L. E. (2010). Tree Species Effects on Ecosystem Water-Use Efficiency in a High-Elevation, Subalpine Forest. *Oecologia*, *162*(2), 491–504. https://doi.org/10.1007/s00442-009-1465-z

Monson, R. K., Turnipseed, A. A., Sparks, J. P., Harley, P. C., Scott-Denton, L. E., Sparks, K., & Huxman, T. E. (2002). Carbon sequestration in a high-elevation, subalpine forest. *Global Change Biology*, *8*(5), 459–478. https://doi.org/10.1046/j.1365-2486.2002.00480.x

Montesi, J., Elder, K., Schmidt, R. A., & Davis, R. E. (2004). Sublimation of intercepted snow within a subalpine forest canopy at two elevations. *Journal of Hydrometeorology*, *5*(5), 763–773. https://doi.org/10.1175/1525-7541(2004)005<0763:soiswa>2.0.co;2

Nakai, Y., Sakamoto, T., Terajima, T., Kitahara, H., & Saito, T. (1994). *Snow interception by forest canopies: Weighing a conifer tree, meteorological observation and analysis by the Penman-Monteith formula* (Vol. 223, pp. 227–236). IAHS Publications-Series of Proceedings and Reports-Intern Assoc Hydrological Sciences.

Nichele, L., Persichetti, V., Lucidi, M., & Cincotti, G. (2020). Quantitative evaluation of ImageJ thresholding algorithms for microbial cell counting. *OSA Continuum*, *3*(6), 1417–1427. https://doi.org/10.1364/OSAC.393971

Niu, G.-Y., & Yang, Z.-L. (2004). Effects of vegetation canopy processes on snow surface energy and mass balances. *Journal of Geophysical Research*, *109*(D23). https://doi.org/10.1029/2004JD004884

Niu, G.-Y., Yang, Z.-L., Mitchell, K. E., Chen, F., Ek, M. B., Barlage, M., et al. (2011). The community Noah land surface model with multiparameterization options (Noah-MP): 1. Model description and evaluation with local-scale measurements. *Journal of Geophysical Research*, *116*(D12), D12109. https://doi.org/10.1029/2010JD015139

O'Brien, H. W., & Munis, R. H. (1975). *Red and near-infrared spectral reflectance of snow*. Corps of Engineers, U.S. Army, Cold Regions Research and Engineering Laboratory.

Parajka, J., Haas, P., Kirnbauer, R., Jansa, J., & Blöschl, G. (2012). Potential of time-lapse photography of snow for hydrological purposes at the small catchment scale. *Hydrological Processes*, *26*(22), 3327–3337. https://doi.org/10.1002/hyp.8389

Phillips, M. (2013). *Estimates of sublimation in the upper Colorado river basin (M.S.)*. Colorado State University. Retrieved from https://www.proquest.com/docview/1496773077/abstract/AD7AA123A1624151PQ/1

Pomeroy, J. W., & Essery, R. L. H. (1999). Turbulent fluxes during blowing snow: Field tests of model sublimation predictions. *Hydrological Processes*, *13*(18), 2963–2975. https://doi.org/10.1002/(SICI)1099-1085(19991230)13:18<2963::AID-HYP11>3.0.CO;2-9

Pomeroy, J. W., & Li, L. (2000). Prairie and arctic areal snow cover mass balance using a blowing snow model. *Journal of Geophysical Research*, *105*(D21), 26619–26634. https://doi.org/10.1029/2000JD900149

Pomeroy, J. W., & Schmidt, R. A. (1993). The use of fractal geometry in modelling intercepted snow accumulation and sublimation. In *Proceedings of the Eastern Snow Conference* (Vol. 50, pp. 1–10).

Raleigh, M. S., Gutmann, E. D., Van Stan II, J. T., Burns, S. P., Blanken, P. D., & Small, E. E. (2022). Challenges and Capabilities in Estimating Snow Mass Intercepted in Conifer Canopies With Tree Sway Monitoring. *Water Resources Research*, *58*(3), e2021WR030972. https://doi.org/10.1029/2021WR030972

Rasouli, K., Pomeroy, J. W., Janowicz, J. R., Carey, S. K., & Williams, T. J. (2014). Hydrological sensitivity of a northern mountain basin to climate change. *Hydrological Processes*, *28*(14), 4191–4208. https://doi.org/10.1002/hyp.10244

Richardson, A. D., Hufkens, K., Milliman, T., Aubrecht, D. M., Chen, M., Gray, J. M., et al. (2018). Tracking vegetation phenology across diverse North American biomes using PhenoCam imagery. *Scientific Data*, *5*(1), 1–24. https://doi.org/10.1038/sdata.2018.28

Roesch, A., Wild, M., Gilgen, H., & Ohmura, A. (2001). A new snow cover fraction parametrization for the ECHAM4 GCM. *Climate Dynamics*, *17*(12), 933–946. https://doi.org/10.1007/s003820100153

Salisbury, J. W., D'Aria, D. M., & Wald, A. (1994). Measurements of thermal infrared spectral reflectance of frost, snow, and ice. *Journal of Geophysical Research*, *99*(B12), 24235–24240. https://doi.org/10.1029/94JB00579

Schaefer, G. L., & Paetzold, R. F. (2001). SNOTEL (SNOwpack TELemetry) and SCAN (soil climate analysis network). In *Presented at the Automated Weather Stations for Applications in Agriculture and Water Resources Management: Current Use and Future Perspective* (pp. 187–194). NB. Retrieved from https://citeseerx.ist.psu.edu/document?repid=rep1&type=pdf&doi=9620e69672ecbc3998ef2760c23765e6f2d242ec

Schmidt, R. A., & Gluns, D. R. (1991). Snowfall interception on branches of three conifer species. *Canadian Journal of Forest Research*, *21*(8), 1262–1269. https://doi.org/10.1139/x91-176

Sexstone, G. A., Clow, D. W., Fassnacht, S. R., Liston, G. E., Hiemstra, C. A., Knowles, J. F., & Penn, C. A. (2018). Snow Sublimation in Mountain Environments and Its Sensitivity to Forest Disturbance and Climate Warming. *Water Resources Research*, *54*(2), 1191–1211. https://doi.org/10.1002/2017WR021172

Seyednasrollah, B., Young, A. M., Hufkens, K., Milliman, T., Friedl, M. A., Frolking, S., & Richardson, A. D. (2019). Tracking vegetation phenology across diverse biomes using Version 2.0 of the PhenoCam Dataset. *Scientific Data*, *6*(1), 1–11. https://doi.org/10.1038/s41597-019-0229-9

Sezgin, M., & Sankur, B. (2004). Survey over image thresholding techniques and quantitative performance evaluation. *Journal of Electronic Imaging*, *13*(1), 146–165. https://doi.org/10.1117/1.1631315

Stähli, M., Jonas, T., & Gustafsson, D. (2009). The role of snow interception in wintertime radiation processes of a coniferous sub-alpine forest. *Hydrological Processes: International Journal*, *23*(17), 2498–2512. https://doi.org/10.1002/hyp.7180

Stigter, E. E., Litt, M., Steiner, J. F., Bonekamp, P. N. J., Shea, J. M., Bierkens, M. F. P., & Immerzeel, W. W. (2018). The importance of snow sublimation on a Himalayan glacier. *Frontiers in Earth Science*, *6*, 108. https://doi.org/10.3389/feart.2018.00108

Strasser, U., Bernhardt, M., Weber, M., Liston, G. E., & Mauser, W. (2008). Is snow sublimation important in the alpine water balance? *The Cryosphere*, *2*(1), 53–66. https://doi.org/10.5194/tc-2-53-2008

Suzuki, K., & Nakai, Y. (2008). Canopy snow influence on water and energy balances in a coniferous forest plantation in northern Japan. *Journal of Hydrology*, *352*(1–2), 126–138. https://doi.org/10.1016/j.jhydrol.2008.01.007

Turnipseed, A. A., Blanken, P. D., Anderson, D. E., & Monson, R. K. (2002). Energy budget above a high-elevation subalpine forest in complex topography. *Agricultural and Forest Meteorology*, *110*(3), 177–201. https://doi.org/10.1016/S0168-1923(01)00290-8

Wang, L., Scott, K. A., & Clausi, D. A. (2017). Sea Ice Concentration Estimation during Freeze-Up from SAR Imagery Using a Convolutional Neural Network. *Remote Sensing*, *9*(5), 408. https://doi.org/10.3390/rs9050408

Yamashita, R., Nishio, M., Do, R. K. G., & Togashi, K. (2018). Convolutional neural networks: An overview and application in radiology. *Insights into Imaging*, *9*(4), 611–629. https://doi.org/10.1007/s13244-018-0639-9

References From the Supporting Information

Bartlett, P. A., MacKay, M. D., & Verseghy, D. L. (2006). Modified snow algorithms in the Canadian land surface scheme: Model runs and sensitivity analysis at three boreal forest stands. *Atmosphere-Ocean*, *44*(3), 207–222. https://doi.org/10.3137/ao.440301

Chen, L., Li, Y., Chen, F., Barr, A., Barlage, M., & Wan, B. (2016). The incorporation of an organic soil layer in the Noah-MP land surface model and its evaluation over a boreal aspen forest. *Atmospheric Chemistry and Physics*, *16*(13), 8375–8387. https://doi.org/10.5194/acp-16-8375-2016

Gao, Y., Li, K., Chen, F., Jiang, Y., & Lu, C. (2015). Assessing and improving Noah-MP land model simulations for the central Tibetan Plateau. *Journal of Geophysical Research: Atmospheres*, *120*(18), 9258–9278. https://doi.org/10.1002/2015JD023404

Jordan, R. (1991). *A one-dimensional temperature model for a snow cover: Technical documentation for SNTHERM.89*. Cold Regions Research and Engineering Lab, U.S. Army Corps of Eng. Retrieved from https://apps.dtic.mil/sti/citations/ADA245493

Lumbrazo, C. (2020). *Evaluating multiple canopy-snow unloading parameterizations in SUMMA with time-lapse photography characterized by citizen scientists*. (Masters Thesis). University of Washington.

Mahat, V., & Tarboton, D. G. (2014). Representation of canopy snow interception, unloading and melt in a parsimonious snowmelt model. *Hydrological Processes*, *28*(26), 6320–6336. https://doi.org/10.1002/hyp.10116

Pomeroy, J. W., Parviainen, J., Hedstrom, N., & Gray, D. M. (1998). Coupled modelling of forest snow interception and sublimation. *Hydrological Processes*, *12*(15), 2317–2337. https://doi.org/10.1002/(sici)1099-1085(199812)12:15<2317::aid-hyp799>3.0.co;2-x

Wang, Z., Zeng, X., & Decker, M. (2010). Improving snow processes in the Noah land model. *Journal of Geophysical Research*, *115*(D20). https://doi.org/10.1029/2009JD013761

Yang, Z.-L., Dickinson, R. E., Robock, A., & Vinnikov, K. Y. (1997). Validation of the Snow Submodel of the Biosphere–Atmosphere Transfer Scheme with Russian Snow Cover and Meteorological Observational Data. *Journal of Climate*, *10*(2), 353–373. https://doi.org/10.1175/1520-0442(1997)010<0353:VOTSSO>2.0.CO;2